

CCDC167 as a potential therapeutic target and regulator of cell cycle-related networks in breast cancer

Pin-Shern Chen^{1,*}, Hui-Ping Hsu^{2,*}, Nam Nhut Phan³, Meng-Chi Yen^{4,5}, Feng-Wei Chen⁶, Yu-Wei Liu¹, Fang-Ping Lin¹, Sheng-Yao Feng¹, Tsung-Lin Cheng^{7,8,9,10}, Pei-Hsiang Yeh¹, Hany A. Omar^{11,12,13}, Zhengda Sun¹⁴, Jia-Zhen Jiang¹⁵, Yi-Shin Chan¹⁶, Ming-Derg Lai^{6,#}, Chih-Yang Wang^{16,17}, Jui-Hsiang Hung^{1,10}

¹Department of Biotechnology, Chia Nan University of Pharmacy and Science, Tainan 70101, Taiwan, Republic of China

²Department of Surgery, National Cheng Kung University Hospital, College of Medicine, National Cheng Kung University, Tainan 70101, Taiwan, Republic of China

³NTT Institute of Hi-Technology, Nguyen Tat Thanh University, Ho Chi Minh 700000, Vietnam

⁴Department of Emergency Medicine, Kaohsiung Medical University Hospital, Kaohsiung Medical University, Kaohsiung 80708, Taiwan, Republic of China

⁵Graduate Institute of Clinical Medicine, College of Medicine, Kaohsiung Medical University, Kaohsiung 80708, Taiwan, Republic of China

⁶Department of Biochemistry and Molecular Biology, Institute of Basic Medical Sciences, College of Medicine, National Cheng Kung University, Tainan 70101, Taiwan, Republic of China

⁷Department of Physiology, School of Medicine, College of Medicine, Kaohsiung Medical University, Kaohsiung 80708, Taiwan, Republic of China

⁸Orthopedic Research Center, College of Medicine, Kaohsiung Medical University Hospital, Kaohsiung Medical University, Kaohsiung 80708, Taiwan, Republic of China

⁹Department of Medical Research, Kaohsiung Medical University Hospital, Kaohsiung Medical University, Kaohsiung 80708, Taiwan, Republic of China

¹⁰Regenerative Medicine and Cell Therapy Research Center, Kaohsiung Medical University, Kaohsiung 80708, Taiwan, Republic of China

¹¹Sharjah Institute for Medical Research and College of Pharmacy, University of Sharjah, Sharjah 27272, United Arab Emirates

¹²Department of Clinical Sciences, College of Pharmacy, Ajman University, Ajman 23000, United Arab Emirates

¹³Department of Pharmacology, Faculty of Pharmacy, BeniSuef University, Beni-Suef 62511, Egypt

¹⁴Kaiser Permanente, Northern California Regional Laboratories, The Permanente Medical Group, Berkeley, CA 94710, USA

¹⁵Emergency Department, Huashan Hospital North, Fudan University, Shanghai 201508, People's Republic of China

¹⁶Graduate Institute of Cancer Biology and Drug Discovery, College of Medical Science and Technology, Taipei Medical University, Taipei 11031, Taiwan, Republic of China

¹⁷PhD Program for Cancer Molecular Biology and Drug Discovery, College of Medical Science and Technology, Taipei Medical University, Taipei 11031, Taiwan, Republic of China

*Equal contribution

#Senior author

Correspondence to: Chih-Yang Wang, Jui-Hsiang Hung; email: chihsyang@tmu.edu.tw, hung86@mail.cnu.edu.tw

Keywords: coiled-coil domain-containing protein 167, breast cancer, cell proliferation, cell growth, bioinformatics

Received: June 25, 2020

Accepted: November 20, 2020

Published: January 10, 2021

Copyright: © 2021 Chen et al. This is an open access article distributed under the terms of the [Creative Commons Attribution License](https://creativecommons.org/licenses/by/3.0/) (CC BY 3.0), which permits unrestricted use, distribution, and reproduction in any medium, provided the original author and source are credited.

ABSTRACT

According to cancer statistics reported in 2020, breast cancer constitutes 30% of new cancer cases diagnosed in American women. Histological markers of breast cancer are expressions of the estrogen receptor (ER), the progesterone receptor (PR), and human epidermal growth factor receptor (HER)-2. Up to 80% of breast cancers are grouped as ER-positive, which implies a crucial role for estrogen in breast cancer development. Therefore, identifying potential therapeutic targets and investigating their downstream pathways and networks are extremely important for drug development in these patients. Through high-throughput technology and bioinformatics screening, we revealed that coiled-coil domain-containing protein 167 (CCDC167) was upregulated in different types of tumors; however, the role of CCDC167 in the development of breast cancer still remains unclear. Integrating many kinds of databases including ONCOMINE, MetaCore, IPA, and Kaplan-Meier Plotter, we found that high expression levels of CCDC167 predicted poor prognoses of breast cancer patients. Knockdown of CCDC167 attenuated aggressive breast cancer growth and proliferation. We also demonstrated that treatment with fluorouracil, carboplatin, paclitaxel, and doxorubicin resulted in decreased expression of CCDC167 and suppressed growth of MCF-7 cells. Collectively, these findings suggest that CCDC167 has high potential as a therapeutic target for breast cancer.

INTRODUCTION

Based on cancer statistics, about 30% of newly diagnosed cancers in the US are breast cancers [1]. According to Immunohistochemical staining results, breast cancer is categorized into different subtypes according to estrogen receptor (ER), progesterone receptor (PR), and human epidermal growth factor receptor (HER)-2. Up to 80% of breast cancer cases are classified as ER-positive (ER⁺), which highlights the significance of estrogen-related signaling in breast cancer [2, 3]. Currently, first-line salvage therapy for tamoxifen-resistant breast cancer patients includes fulvestrant (a selective ER down-regulator) [4, 5], cyclin-dependent kinase 4/6 (CDK4/6) inhibitors [6], aromatase inhibitors, everolimus (a mammalian target of rapamycin inhibitor) [7], and histone deacetylase (HDAC) inhibitors [8]. However, resistance to these salvage therapies ultimately develops, and patients die from their cancer [9, 10]. Therefore, it is important to explore new effective therapeutics for ER⁺ breast cancer patients. Coiled-coil domain (CCD) constituents are alpha-helix motifs expressed in different types of proteins. Owing to structural flexibility, they can function in various biological processes, including cell proliferation, migration, and signal transduction [11, 12]. In recent publications, CCD-containing (CCDC) proteins were aberrantly activated in multiple types of tumors, including CCDC178 in liver cancer, CCDC88A in pancreatic cancer, and CCDC8 in lung cancer [13–18]. In addition, CCDC106 promotes the proliferation of lung cancer cell lines, and CCDC34 contributes to colorectal cancer development by inhibiting apoptosis signaling and promoting invasion [19]. Inhibition of CCDC69 increases platinum-induced apoptosis in A2780 ovarian cancer cells [20]. Knockdown of CCDC106 enhances apoptosis and suppresses growth of

MCF7 breast cancer by stabilizing p53 [21]. However, there is yet little knowledge of the role of CCDC167 in breast cancer development.

Differential gene expression analyses in high-throughput techniques, such as RNA-sequencing (RNA-Seq), are performed by comparing gene expression profiles between two different conditions. The results define a set of genes with high expressions in cancer and low expressions in normal tissue through statistical tests [22–26]. However, in some particular circumstances, non-differentially expressed genes can contribute to disease dysfunction through clusters of co-expressed genes. These genes may manifest their functions through interaction networks with other differentially expressed genes. Therefore, expression signatures of these co-expressed genes might be crucial factors indirectly affecting the disease condition [27–31]. In the present study, we used a meta-analysis approach combined with a literature review to explore potential therapeutic targets in breast cancer. We systematically investigated messenger (m)RNA expression of CCDC167 and the survival probability of ER⁺ breast cancer patients using a public high-throughput database. Meanwhile, we also investigated the effects of CCDC167 on the progression of breast cancer with an experimental approach.

RESULTS

Increased expression of CCDC167 in breast cancer patients

Transcription expression levels of CCDC167 in 20 types of cancer were screened in the Oncomine database. The CCDC167 gene was upregulated in breast cancer compared to normal tissues in 12 studies

was a correlation between CCDC167 and histological differentiation of breast cancer, with increasing expression levels of CCDC167 as tumors progressed from nuclear grade I to III (Figure 1E). The bioinformatics analysis of breast cancer patient samples collectively provided clues to a potential role of CCDC167 during breast cancer development.

CCDC167 regulates cancer development via cell cycle-related pathways

The role of CCDC167 in breast cancer has been less well studied, therefore, in the present study, we used co-expression analyses to reveal biological functions and information of possible mechanisms. Co-expression profiles of CCDC167 from breast cancers were identified in the METABRIC and TCGA databases. MetaCore analysis of GO enrichment was performed to predict gene functions and regulatory patterns (Figure 2). We merged results from METABRIC and TCGA to obtain common co-expressed genes, which were then

imported into the MetaCore platform. Results of pathway maps indicated that cell cycle-related signaling plays an essential role in breast cancer according to both databases (Supplementary Table 1). We discovered that genes co-expressed with CCDC167 also affected immune- and ubiquinone-related pathways, including “immune response antigen presentation by MHC class I”, “immune response interferon (IFN)-alpha/beta signaling via phosphatidylinositol 3-kinase (PI3K) and nuclear factor (NF)-κB pathways”, and “ubiquinone metabolism” in breast cancer.

In addition, from both TCGA and METABRIC databases, we found that “cell cycle role of the anaphase-promoting complex (APC) in cell cycle regulation” was the most significantly regulated pathway by CCDC167 co-expression in breast cancer (Figure 3). We also identified several miRNAs through the miRWalk and IPA databases, including hsa-mir-760, hsa-mir-1193, hsa-mir-3960, hsa-miR-214-3p, hsa-miR-204-5p, hsa-miR-370-3p, hsa-miR-423-5p, and

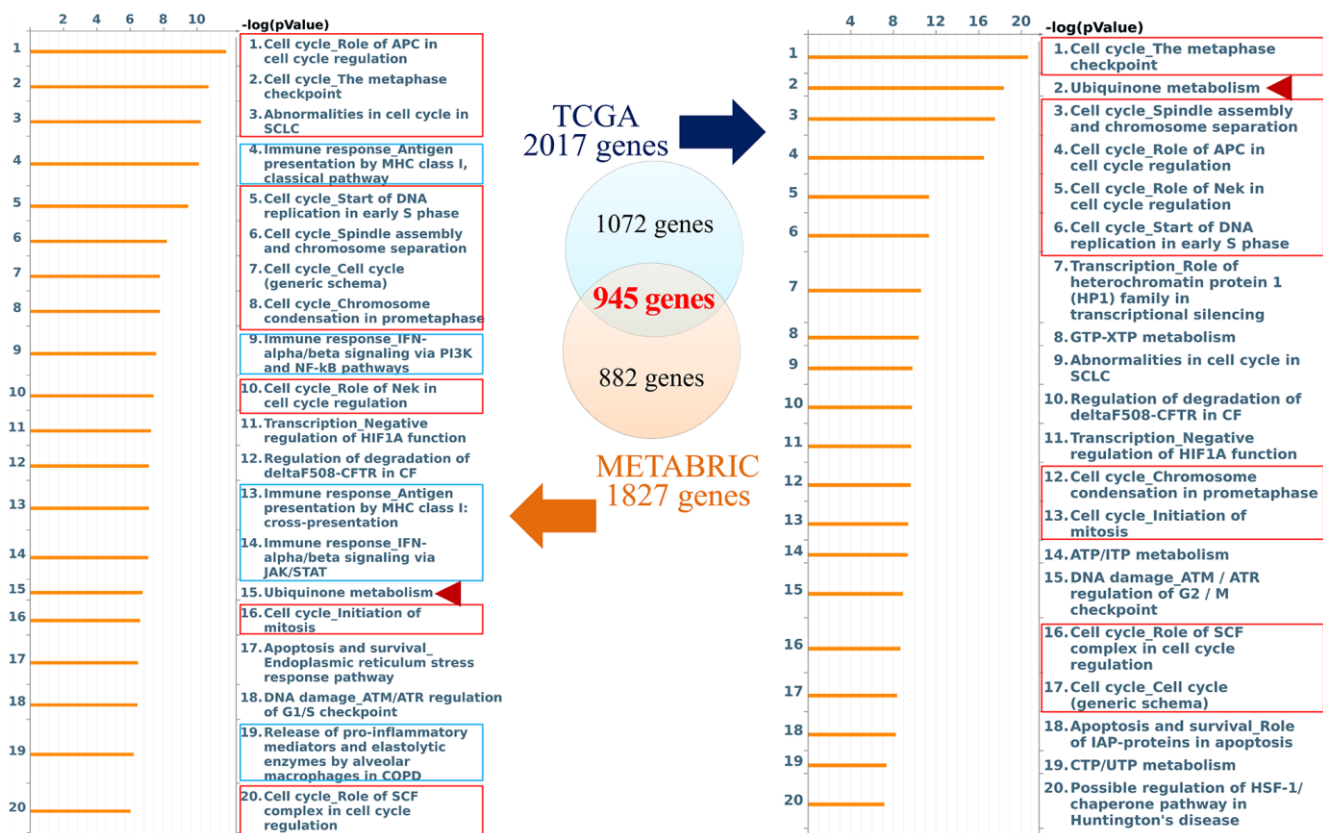


Figure 2. Networks from coiled-coil domain-containing protein 167 (CCDC167)-co-expressed genes in breast cancer. The Venn diagram circles represent co-expressed genes of CCDC167 from each database; the blue circle represents co-expressed genes in TCGA database, and the orange circle represents co-expressed genes in the METABRIC database. The MetaCore signaling pathway analysis demonstrated that the “cell cycle role of anaphase-promoting complex (APC) in cell cycle regulation” and cell cycle-related signaling (red rectangles) were significantly correlated with CCDC167 gene expression. Immune-response signaling is marked with blue rectangles, and ubiquinone metabolism is scored with red arrowheads.

hsa-miR-744-5p, which may interact with CCDC167 (Figure 4).

Downregulation of CCDC167 inhibits the growth of MCF-7 cells

We further investigated the effect of increased expression of CCDC167 on carcinogenesis-related

processes, such as proliferation, migration, and anchorage-independent growth. M10 (non-tumorigenic), MCF-7 (ER+ subtype), MDA-MB-231 (triple-negative subtype), and MDA-MB-468 (highly invasive) cell lines are widely used for breast cancer research, and they represent different subtypes [32, 33]. Therefore, we chose these four cell lines for further study. Endogenous levels of CCDC167 differed

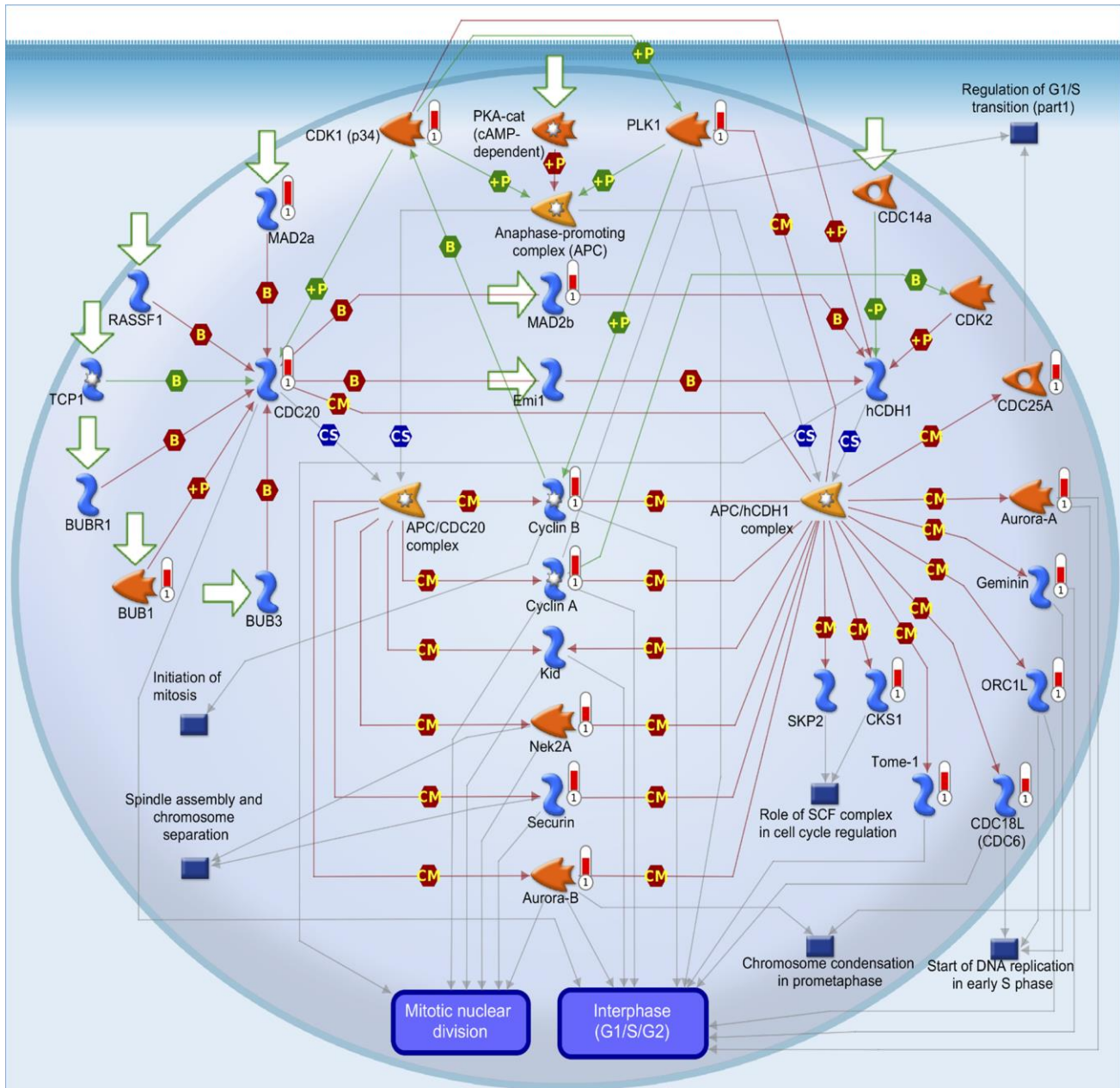


Figure 3. MetaCore pathway analysis of coiled-coil domain-containing protein 167 (CCDC167)-co-expressed genes in breast cancer patient databases. CCDC167-co-expressed genes in breast cancer from TCGA and METABRIC databases were acquired and identified by the Venn diagram analysis in Figure 2. These 945 genes were further exported to the MetaCore pathway analysis tool to identify gene networks and signaling pathways. The “cell cycle role of anaphase-promoting complex (APC) in cell cycle regulation” was the most significantly associated pathway. APC forms a complex with cell division cycle 20 (CDC20) or cadherin-1 (CDH1) to regulate the cell cycle.

in a variety of breast cancer cell lines. We used a qPCR to detect CCDC167 mRNA levels, and results showed the highest expression of CCDC167 in MCF-7 cells compared to other breast cancer cell lines (Figure 5A). Plasmids of CCDC167-shRNA and the vector control from RNAi Core were transfected into the MCF-7 cell line. The knockdown efficiency of shRNA on exogenous CCDC167 was examined by a qPCR. A significant reduction in CCDC167 mRNA expression was observed upon transfection with the shCCDC167 plasmid (Figure 5B).

In order to investigate the anti-proliferative effect of CCDC167 shRNA on human breast MCF-7 cancer cells, we first measured its cell proliferation ability. The MTT assay detected differences in short-term cell proliferation between CCDC167-knockdown and

control MCF-7 cells (Figure 5C). The long-term ability of cell proliferation was examined by a colony-formation assay. Long-term cell growth was suppressed in CCDC167-shRNA cells (Figure 5D), and the difference compared to control cells was significant (Figure 5E). Meanwhile, the ability to form colonies was higher in CCDC167-overexpressing MCF-7 cells, and the results confirmed that overexpression of CCDC167 promoted cell proliferation (Supplementary Figure 2A). Knockdown of CCDC167 significantly altered cell cycle-related and apoptosis-related genes (Supplementary Figure 2B). Percentages of both early and late apoptosis increased after CCDC167-knockdown (Supplementary Figure 3). Meanwhile, in order to investigate gene expressions of other CCDC family members in the METABRIC database, we also compared mRNA expression levels between different

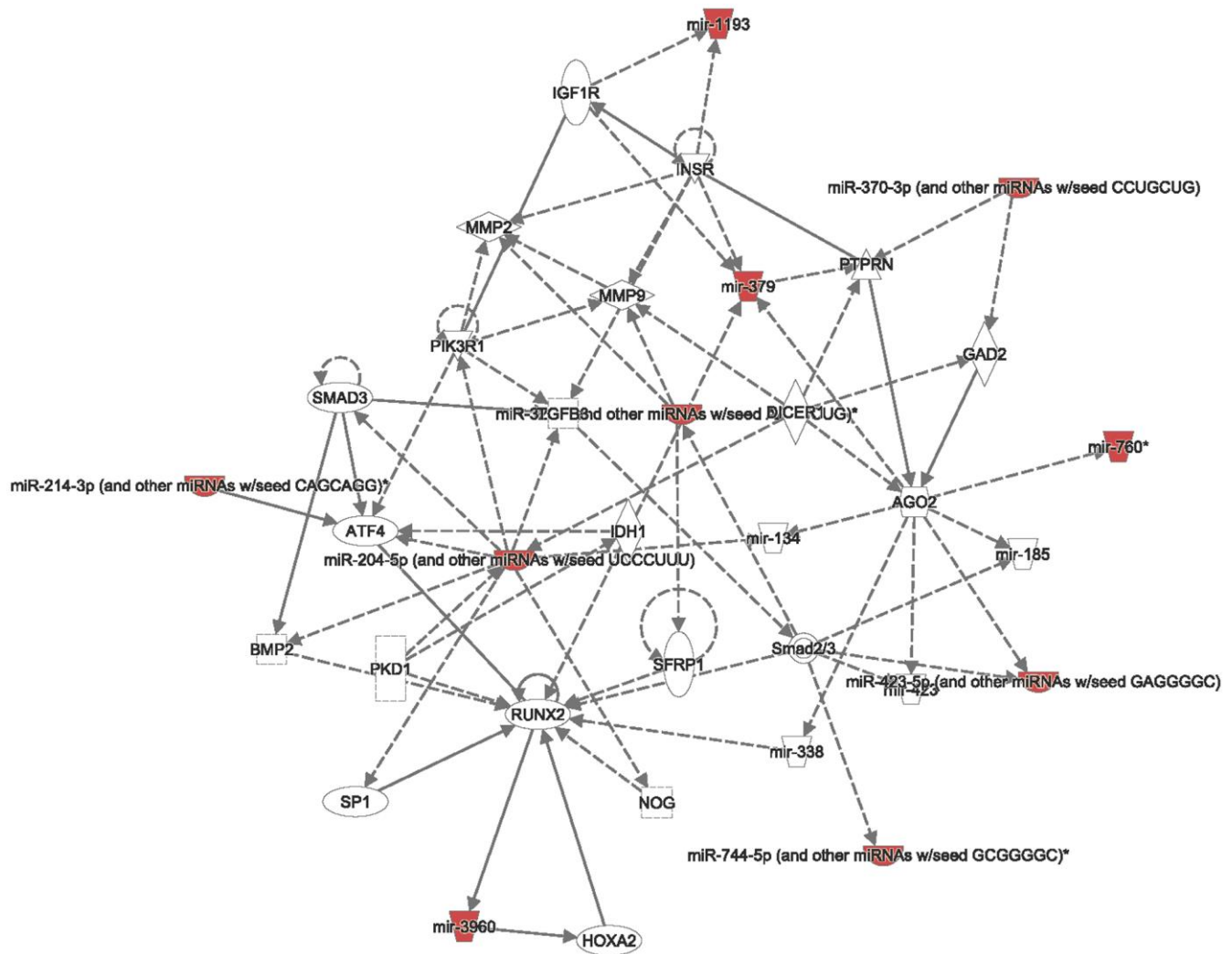


Figure 4. Interacting networks between coiled-coil domain-containing protein 167 (CCDC167) and micro (mi)RNA. The miRWalk database analyzed CCDC167-interacting miRNAs, and then the related networks were analyzed by an Ingenuity Pathway Analysis (IPA). These miRNAs and CCDC167-co-expressed genes are critical to the progression of breast cancer.

subtypes of breast cancer including claudin-low, basal, Her2, luminal A, and luminal B relative to normal breast tissues (Supplementary Figures 4–10). Several CCDC members were significantly overexpressed in breast cancer subtypes, which might imply the high impact of CCDC family genes on tumor development.

The survival status and clinical application of CCDC167

Fluorouracil (5-FU), carboplatin, paclitaxel, and doxorubicin are currently first- or second-line cytotoxic

agents of adjuvant chemotherapy for breast cancer patients. Treatments with these compounds resulted in decreased cellular growth of MCF-7 cells (Figure 6A). Based on the qPCR results, we also found that treatment with these compounds also significantly decreased CCDC167 mRNA expression, which suggested that these drugs may downregulate CCDC167 signaling in breast cancer progression (Figure 6B).

We further analyzed CCDC167 overexpression in breast cancer patients (Figure 6C). Data on recurrence-free survival (RFS) and overall survival (OS) of breast cancer

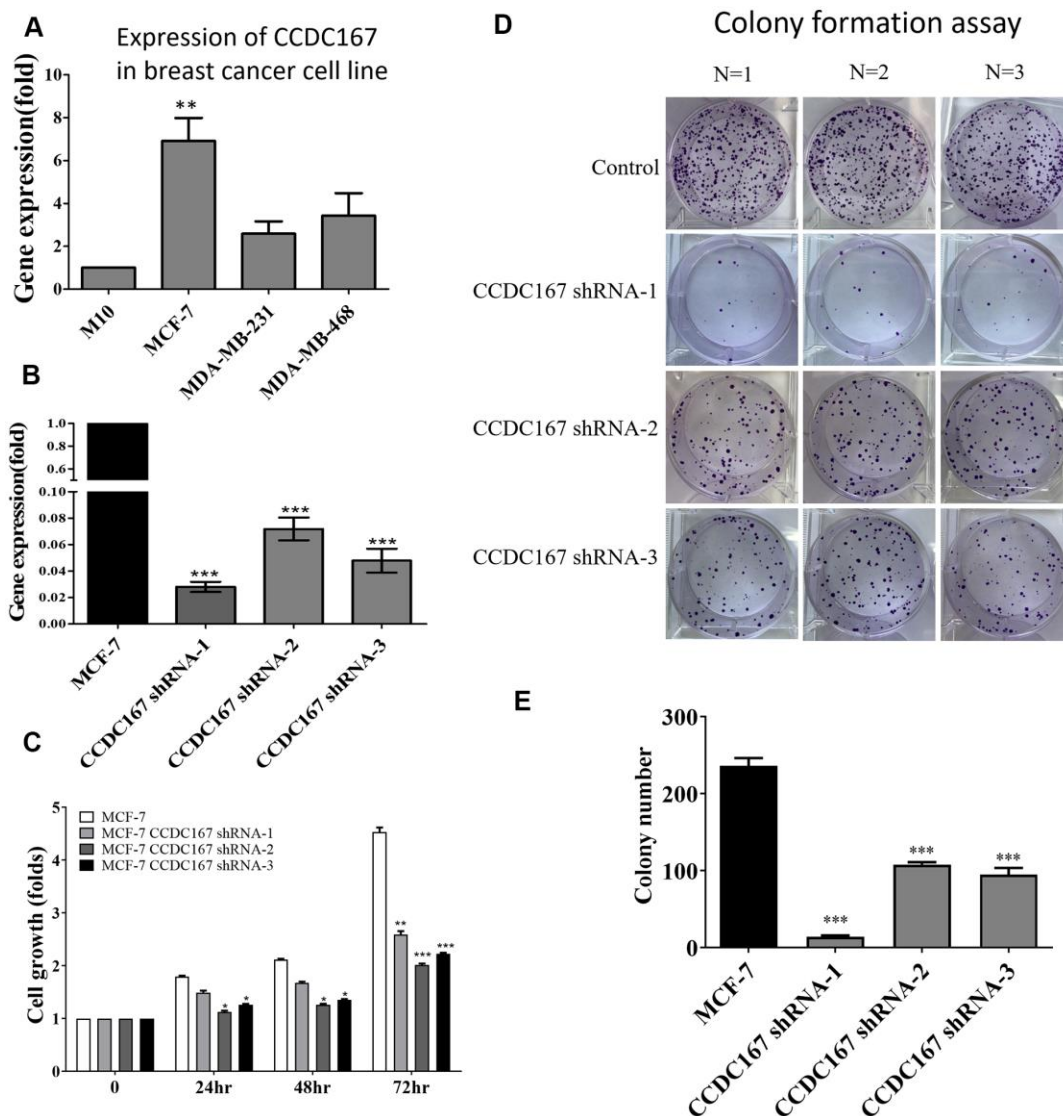


Figure 5. Coiled-coil domain-containing protein 167 (CCDC167)-knockdown by shRNA significantly attenuated the proliferation of MCF-7 breast cancer cells. (A) The mRNA expression of CCDC167 was determined in a variety of breast cancer cell lines. (B) A qPCR analyzed CCDC167 mRNA expression in shCCDC167-knockdown cells. (C) Evaluation of the growth of shCCDC167-knockdown and vector control MCF-7 cells according to MTT assays. (D) A colony-formation assay determined proliferation rates of the MCF-7 vector control and stable shCCDC167-knockdown MCF-7 cells. (E) Statistical data of the colony-formation assay. Values are the average of assays performed in triplicate. The standard deviation is displayed using error bars ($n=3$). * $p<0.05$.

patients were collected from the Kaplan-Meier Plotter database. High expression of CCDC167 was correlated with worse RFS and OS. High expression of CCDC167 was also correlated with RFS in the GSE25307 datasets [34] and disease-specific survival in the GSE3494 datasets [35, 36]. All of these results demonstrated that high expression of CCDC167 predicted poor prognoses.

DISCUSSION

Integrated analyses from this study showed that the CCDC167 expression level was higher in breast cancer. TCGA and METABRIC databases were used to analyze potentially CCDC167-co-expressed genes in breast cancer. We also used the MCF-7 breast cancer cell line and performed short-term and long-term cell proliferation assays to validate our bioinformatics pre-

dictions. CCDC167 expression has the potential to predict the survival of breast cancer patients and provide targets for further therapy. To the best of our knowledge, the present study is the first to provide comprehensive evidence of a novel association between CCDC167 and the prognosis of breast cancer patients.

The differential co-expression concept is related to gene-gene comparisons between two conditions, such as cancer and normal tissues. It implies that any alterations detected by conventional methods for differentially expressed genes might do not be beneficial if some genes not pass the differential threshold. However, insignificant changes in these genes could indirectly affect the regulatory system due to their co-expressed genes [37–39]. These differentially co-expressions could contribute to the disease without changing their expression levels. These differentially co-expressed genes and their

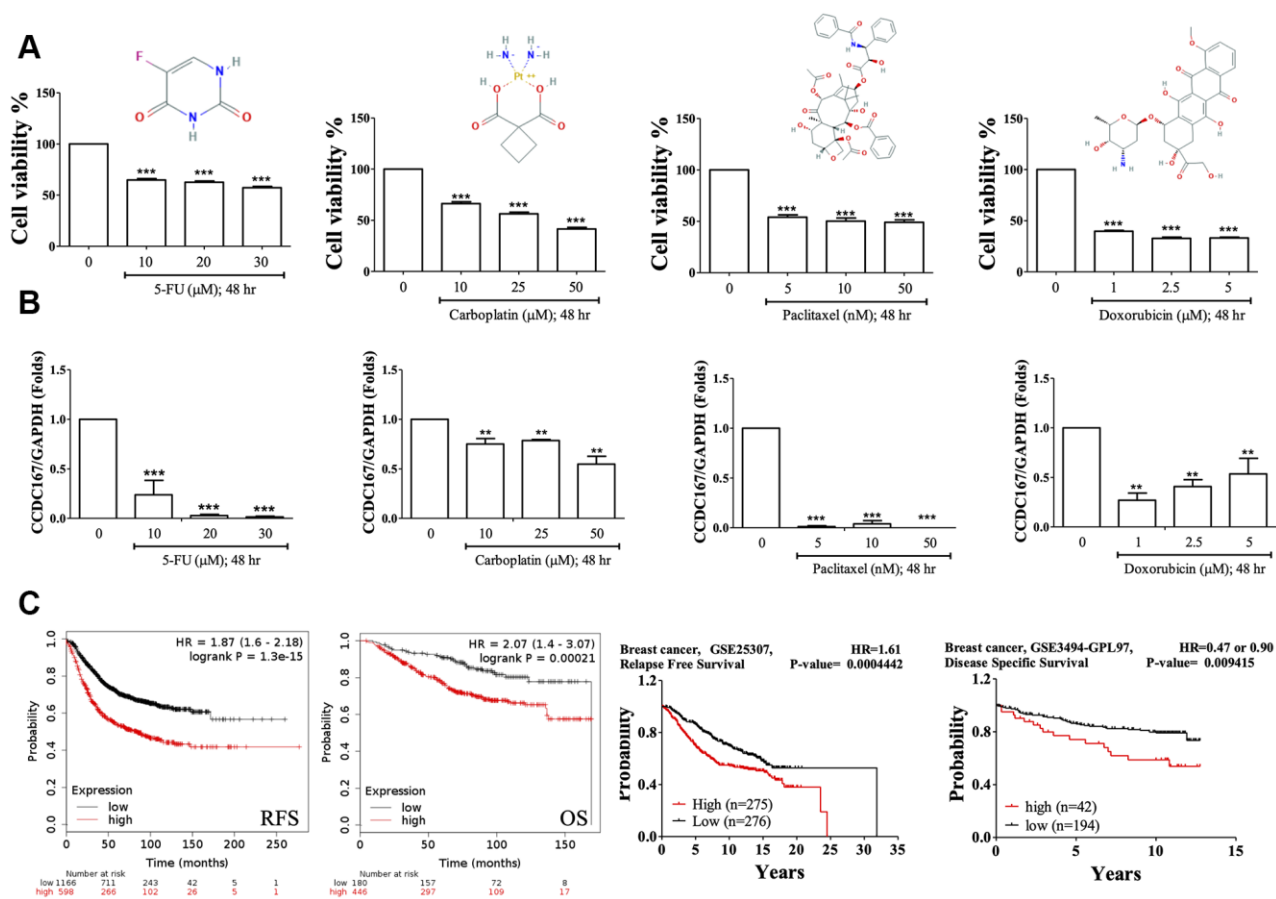


Figure 6. Drug testing for breast cancer cell lines and the survival of breast cancer patients. (A) Fluorouracil (5-Fu), carboplatin, paclitaxel, and doxorubicin treatments resulted in decreased cellular growths in MTT assays of MCF-7 cells. (B) Coiled-coil domain-containing protein 167 (CCDC167) mRNA alterations when treated with 5-Fu, carboplatin, paclitaxel, and doxorubicin for 2 days. (* $p < 0.05$ was considered significant). (C) Correlation of CCDC167 recurrence-free survival and overall survival in Kaplan-Meier Plotter, using the GSE25307 dataset for recurrence-free survival and the GSE3494-GPL97 dataset for disease-specific survival in breast cancer patients. The red lines indicate high transcriptional expression levels of CCDC167, whereas the black lines indicate low expression levels. The plots also display hazard ratios (HRs), with 95% confidence intervals (CIs) and log-rank p values. High expression levels of CCDC167 predicted poor prognoses.

associated disease can be revealed using gene-gene correlations between cancer and normal tissues. This information could potentially be useful in combination with conventional analyses of differential expression patterns. In addition, it could help identify underlying mechanisms in a biological system under different conditions. Detailed mechanisms of the CCDC167 gene in breast cancer were explored by examining its co-expressed genes from TCGA and METABRIC databases. Afterward, GeneGo and MetaCore annotations for enriched biological processes indicated that CCDC167-co-expressed genes were involved in cell cycle-related molecular processes. Next, in order to validate our bioinformatics predictions, we measured the ability of cells to proliferate with both a short-term MTT assay and a long-term colony-formation assay. MCF-7 shCCDC167 cells exhibited a significantly lower ability of cell proliferation compared to vector control cells.

Furthermore, we found that CCDC167-co-expressed genes were also involved in cell cycle and ubiquitination pathways, highlighting their essential roles in breast cancer. Cell division progression, ubiquinone metabolism, initiation of mitosis, spindle assembly, and chromosome separation were all top-ranked pathways of CCDC167-co-expressed genes. These results were found in the METABRIC and TCGA-BRCA datasets, and the findings were consistent across different populations. CCDC167-co-expressed genes were involved in the cell cycle, immune response, and ubiquitination-related pathways. CCDC167 also cooperated with several miRNA and oncogenic signaling pathways. The high expression of CCDC167 in breast cancer patients was also correlated with worse survival in these public databases. All of these data implicated the significance of CCDC167 in the progression of breast cancer. 5-FU, carboplatin, paclitaxel, and doxorubicin have the ability to inhibit breast cancer cell growth. These US FDA-approved compounds are currently first- or second-line regimens for postoperative adjuvant chemotherapy of breast cancer patients. We also found that treatment with fluorouracil, carboplatin, paclitaxel, and doxorubicin resulted in decreased expression of CCDC167 and suppressed growth of MCF-7 cells; these data suggested that CCDC167 signaling might be a critical target for these cytotoxic drugs. Other compounds that act against CCDC167 could be new therapeutic agents for treating breast cancer patients.

In conclusion, the present study demonstrated the crucial roles played by CCDC167 and its downstream signaling in breast cancer patients. These CCDC167-related pathways could potentially be targeted for treating and preventing breast cancer. The current study focused on CCDC167 pathways and cell cycle-related signatures,

and these findings suggest that CCDC167 could have high potency as targeted therapy for breast cancer.

MATERIALS AND METHODS

Cell culture, and 3-(4,5-dimethylthiazol-2-yl)-2,5-diphenyltetrazolium bromide (MTT) and colony-formation assays

MCF-7 cells were grown in 10% fetal bovine serum (FBS) supplemented with Dulbecco's modified Eagle's medium (DMEM). The ability for short-term cell proliferation was examined by an MTT assay. A colony-formation assay was utilized to evaluate the ability of long-term cell proliferation. MCF-7 cells were trypsinized and seeded in six-well plates at a low density of 500 cells/well and grown in the presence of US Food and Drug Administration (FDA)-approved drugs predicted from a bioinformatics analysis [40–45]. After 2 weeks, the medium was aspirated from the six-well plates, and MCF-7 cells were fixed with methanol. Then, 0.1% crystal violet in distilled water was added to each well for 10 min to stain the colonies. After the crystal violet solution was removed, the plates were washed with distilled water five times and air-dried. Colonies in each well were enumerated under low-magnification light microscopy.

Determination of mRNA expression using a reverse-transcription quantitative polymerase chain reaction (RT-qPCR)

We used TRIzol reagent (Invitrogen, Carlsbad, CA, USA) for total RNA extraction from MCF-7 cells following a datasheet. Next, a cDNA Reverse Transcription Kit (Applied Biosystems, Carlsbad, CA, USA) was used for reverse transcription of total RNA (1 µg) to complementary (c)DNA. A real-time PCR with the FastStart Universal SYBR Green Master (Roche, Basel, Switzerland) kit was conducted with 5% of each cDNA as the template with the ABI Step One Plus system (Applied Biosystems). Each experiment was repeated three times, and all results were normalized to GAPDH [46–51]. For small hairpin (sh)RNA-mediated signaling, shRNAs targeting CCDC167 and vector control were purchased from the National RNAi Core Facility (Academia Sinica, Taipei, Taiwan; <http://rna.genmed.sinica.edu.tw>) according to accession no. TCRN0000140864 with target sequence 5' -CCG GCC TAG TGT TCA AGC ATG GCT TCT CGA GAA GCC ATG CTT GAA CAC TAG GTT TTT TG-3'; no. TCRN0000142200 with target sequence 5' -CCG GGA AGT TTC TTC GGC AAG AGA ACT CGA GTT CTC TTG CCG AAG AAA CTT CTT TTT TG-3'; and TCRN0000122824 with target sequence 5' -CCG GGC CTA ATG AAC AAA GCC TCC ACT CGA GTG GAG GCT TTG TTC ATT AGG CTT TTT

TG-3'. A control construct (pLKO.1 containing luciferase non-silenced shRNA) was also purchased from the National RNAi Core Facility as an expression control. The following human primers for the qPCR were used in this study: human CCDC167 forward 5' - AGA CCT GGA GGC CGT GAA CT-3' and reverse 5' -AGA CCT GGA GGC CGT GAA CT-3'; GAPDH forward 5'-GAT TCC ACC CAT GGC AAA TTC-3' and reverse 5'-AGC ATC GCC CCA CTT GAT T-3'; RIPK1 forward 5'-GCA CCG CTA AGA AGA ATG G -3' and reverse 5'-GCC ACA CAA TCA AGT TGA AGA G-3'; Fas forward 5'-GAC CCA GAA TAC CAA GTG CAG-3' and reverse 5'-GTT CTG CTG TGT CTT GGA CAT TGT C-3'; caspase-3 forward 5'-TGG CAT ACT CCA CAG CAC CTG GTT A-3' and reverse 5'-CAT GGC ACA CAA AGC GAC TGG ATG AA-3'; cytochrome-c forward 5'-TTT GGA TCC AAT GGG TGA TGT TGA G-3' and reverse 5'-TTT GAA TTC CTC ATT AGT AGC TTT TTT GAG-3'; Bax forward 5'-TGC TTC AGG GTT TCA TCC AG-3' and reverse 5'-GGC GGC AAT CAT CCT CTG-3'; and tumor necrosis factor (TNF)- α forward 5'-TGC TTC AGG GTT TCA TCC AG-3' and reverse 5'-GGC GGC AAT CAT CCT CTG-3'.

Cell cycle assessment of CCDC167-knockdown in MCF-7 cells by flow cytometry

For the cell cycle assay, CCDC167 knockdown MCF-7 cells and the parental cells were grown in 10 cm dish, then we used trypsin to isolate cell. Next, the cells were centrifuged for 5 min at 1000 \times g, fixed with 70 % alcohol as well as ice-cold PBS, and incubated at 40° C for a minimum of 30 min. RNase (Takara, Shiga, Japan) was added to the samples within 30 min at room temperature. The propidium iodide (PI) solution and Annexin V-FITC Apoptosis Kit (AAT Bioquest, Inc. CA, USA) and was used for cell cycle experiments. All samples were analyzed using flow cytometry (FACS Calibur; BD Biosciences, San Jose, CA, USA) with a counting threshold of 10⁶ cells.

Analyses of CCDC167 gene expression in multiple types of cancers in the Oncomine and gene expression profiling interactive analysis (GEPIA)

Transcriptomics expression levels of CCDC167 in multiple types and subtypes of cancers were screened in the Oncomine database with public high-throughput datasets using differential analysis options for cancer versus normal samples in the primary filters [52]. The method was clearly described in our previous studies [53–57]. Briefly, the thresholds for *p* values, multiples of change, and gene rank percentiles were set to 0.001, 1.5, and the top 10%, respectively. For the co-expression analysis, we selected breast cancer-related datasets which

satisfied the thresholds mentioned above. The dataset with the highest correlation score was selected for analysis of genes co-expressed with CCDC167. In addition to the Oncomine database, we also used the GEPIA to analyze mRNA expression levels of CCDC167 in 33 datasets available in The Cancer Genome Atlas (TCGA) database [58]. CCDC167 expression levels were compared between tumor and normal groups, and these comparisons are illustrated in a dot plot with a log₂ scale of transcripts per million (TPM) [59].

Bioinformatics, functional enrichment analysis, and micro (mi)RNA-regulated networks

The RNA-Seq dataset from TCGA [60] and Molecular Taxonomy of Breast Cancer International Consortium (METABRIC) [61] were retrieved from the cBioPortal [62]. Normalized expression data were used to obtain the top 10% co-expressed genes based on CCDC167 expression, and a Venn diagram was plotted to determine genes highly correlated with CCDC167. Finally, these co-expressed genes were further analyzed using networks and pathways. The molecular functions and disease pathways of Gene Ontology (GO) terms in MetaCore (GeneGo, St. Joseph, MN, USA) were used to screen and analyze signaling networks in these breast cancer patients [63–66]. A *p* value of <0.05 represented statistical significance. To search for CCDC167-associated miRNAs, we used miRWalk 2.0 to predict potentially regulated miRNAs. Based on the miRmap score, which was calculated as the repressive strength of miRNA binding to its target mRNA, we chose a cutoff of the miRmap score of >99 for inclusion in our study and analyzed regulated pathways and networks with an Ingenuity Pathway Analysis (IPA).

mRNA expressions of CCDC family members in different subtypes of breast cancer

Expression data from CCDC family genes were collected from the METABRIC database and plotted with a violin plot for comparisons among different molecular subtypes, including basal, claudin-low, HER-2, luminal A, luminal B, and normal-like breast cancers. Plots were conducted with R studio vers. 1.2.1335 under R vers. 4.0.3 using the ggpubr package vers. 0.4.0 [67].

Analysis of survival probability

Correlations of mRNA expression levels of CCDC167 and breast cancer patient survival were analyzed using the Kaplan Meier-plot database [68]. In brief, distant metastasis-free survival (DMFS) was selected for CCDC167 with all default settings of the Kaplan Meier-Plot database to obtain the survival curve. In addition, survival data of the GSE25307 and GSE3494-GPL97

datasets were downloaded from the NCBI GEO and PrognScan databases, and the survival risk was calculated using the Kaplan-Meier method with the log-rank test.

Statistical analysis

All results are reported as the mean \pm standard deviation (SD) with three or more replicates. Student's *t*-test was used to calculate differences between groups with $p < 0.05$ accepted as significant.

AUTHOR CONTRIBUTIONS

Conceptualization, P.S.C., H.P.H., M.D.L., C.Y.W., and J.H.H.; methodology, Y.W.L., F.P.L., and S.Y.F.; software, T.L.C., P.H.Y., and H.A.O.; validation, N.N.P., Z.S., and M.D.L.; formal analysis, P.S.C., M.C.Y., F.W.C., Y.S.C., and H.P.H.; investigation, H.P.H., M.D.L., C.Y.W., and J.H.H.; resources, J.Z.J.; data curation, Y.W.L., M.C.Y., and F.W.C.; writing, original draft preparation, P.S.C. and H.P.H.; writing, review and editing, M.D.L., C.Y.W., and J.H.H.; visualization, P.S.C. and H.P.H.; supervision, M.D.L., C.Y.W., and J.H.H.; project administration, M.D.L., C.Y.W., and J.H.H.; and funding acquisition, H.P.H., M.D.L., C.Y.W., and J.H.H. All authors have read and agreed to the published version of the manuscript.

ACKNOWLEDGMENTS

The authors give special thanks to Prof. Ju-Ming Wang from National Cheng Kung University for his technical support, and we would like to thank Mr. Daniel P. Chamberlin for his professional English editing from the Office of Research and Development at Taipei Medical University.

CONFLICTS OF INTEREST

The authors declare no conflicts of interest.

FUNDING

Bioinformatics analyses and data mining were conducted at Taipei Medical University. The study was supported by the Ministry of Science and Technology (MOST) of Taiwan (grants MOST105-2325-B-006-003 to M-D.L., and MOST 108-2314-B-006-082 to H-P. H., and MOST109-2320-B-038-009-MY2 to C-Y.W., and MOST108-2320-B-041-002, 109-2320-B-041-001 to J-H.H.), National Cheng Kung University Hospital (grant NCKUH-10601002 to M-D.L.), and Taipei Medical University (grant TMU-108-AE1-B16 to C-Y.W.). This research was supported in part by Higher Education Sprout Project, Ministry of Education to the Headquarters of University Advancement at NCKU.

REFERENCES

1. Siegel RL, Miller KD, Jemal A. Cancer statistics, 2020. *CA Cancer J Clin.* 2020; 70:7–30. <https://doi.org/10.3322/caac.21590> PMID:31912902
2. Robinson DR, Wu YM, Vats P, Su F, Lonigro RJ, Cao X, Kalyana-Sundaram S, Wang R, Ning Y, Hodges L, Gursky A, Siddiqui J, Tomlins SA, et al. Activating ESR1 mutations in hormone-resistant metastatic breast cancer. *Nat Genet.* 2013; 45:1446–51. <https://doi.org/10.1038/ng.2823> PMID:24185510
3. Li AQ, Zhou SL, Li M, Xu Y, Shui RH, Yu BH, Yang WT. Clinicopathologic Characteristics of Oestrogen Receptor-Positive/Progesterone Receptor-Negative/Her2-Negative Breast Cancer According to a Novel Definition of Negative Progesterone Receptor Status: A Large Population-Based Study from China. *PLoS One.* 2015; 10:e0125067. <https://doi.org/10.1371/journal.pone.0125067> PMID:25938238
4. Nardone A, Weir H, Delpuech O, Brown H, De Angelis C, Cataldo ML, Fu X, Shea MJ, Mitchell T, Veeraraghavan J, Nagi C, Pilling M, Rimawi MF, et al. The oral selective oestrogen receptor degrader (SERD) AZD9496 is comparable to fulvestrant in antagonising ER and circumventing endocrine resistance. *Br J Cancer.* 2019; 120:331–39. <https://doi.org/10.1038/s41416-018-0354-9> PMID:30555156
5. Chen SH, Cheung CHA. (2018). Challenges in Treating Estrogen Receptor-Positive Breast Cancer. *Estrogen: IntechOpen.* <https://doi.org/10.5772/intechopen.79263>
6. Finn RS, Aleshin A, Slamon DJ. Targeting the cyclin-dependent kinases (CDK) 4/6 in estrogen receptor-positive breast cancers. *Breast Cancer Res.* 2016; 18:17. <https://doi.org/10.1186/s13058-015-0661-5> PMID:26857361
7. Burris HA 3rd. Overcoming acquired resistance to anticancer therapy: focus on the PI3K/AKT/mTOR pathway. *Cancer Chemother Pharmacol.* 2013; 71:829–42. <https://doi.org/10.1007/s00280-012-2043-3> PMID:23377372
8. Munster PN, Thurn KT, Thomas S, Raha P, Lacevic M, Miller A, Melisko M, Ismail-Khan R, Rugo H, Moasser M, Minton SE. A phase II study of the histone deacetylase inhibitor vorinostat combined with tamoxifen for the treatment of patients with hormone therapy-resistant breast cancer. *Br J Cancer.* 2011;

- 104:1828–35.
<https://doi.org/10.1038/bjc.2011.156> PMID:[21559012](https://pubmed.ncbi.nlm.nih.gov/21559012/)
9. Davies C, Godwin J, Gray R, Clarke M, Cutter D, Darby S, McGale P, Pan HC, Taylor C, Wang YC, Dowsett M, Ingle J, Peto R, and Early Breast Cancer Trialists' Collaborative Group (EBCTCG). Relevance of breast cancer hormone receptors and other factors to the efficacy of adjuvant tamoxifen: patient-level meta-analysis of randomised trials. *Lancet*. 2011; 378:771–84.
[https://doi.org/10.1016/S0140-6736\(11\)60993-8](https://doi.org/10.1016/S0140-6736(11)60993-8)
PMID:[21802721](https://pubmed.ncbi.nlm.nih.gov/21802721/)
 10. Bezerra LS, Santos-Veloso MA, Bezerra Junior ND, Fonseca LC, Sales WL. Impacts of cytochrome P450 2D6 (CYP2D6) genetic polymorphism in tamoxifen therapy for breast cancer. *Rev Bras Ginecol Obstet*. 2018; 40:794–99.
<https://doi.org/10.1055/s-0038-1676303>
PMID:[30536272](https://pubmed.ncbi.nlm.nih.gov/30536272/)
 11. Qian F, Germino FJ, Cai Y, Zhang X, Somlo S, Germino GG. PKD1 interacts with PKD2 through a probable coiled-coil domain. *Nat Genet*. 1997; 16:179–83.
<https://doi.org/10.1038/ng0697-179> PMID:[9171830](https://pubmed.ncbi.nlm.nih.gov/9171830/)
 12. Tanner MJ, Hanel W, Gaffen SL, Lin X. CARMA1 coiled-coil domain is involved in the oligomerization and subcellular localization of CARMA1 and is required for T cell receptor-induced NF-kappaB activation. *J Biol Chem*. 2007; 282:17141–47.
<https://doi.org/10.1074/jbc.M700169200>
PMID:[17428801](https://pubmed.ncbi.nlm.nih.gov/17428801/)
 13. Hu X, Zhao Y, Wei L, Zhu B, Song D, Wang J, Yu L, Wu J. CCDC178 promotes hepatocellular carcinoma metastasis through modulation of anoikis. *Oncogene*. 2017; 36:4047–59.
<https://doi.org/10.1038/onc.2017.10> PMID:[28319061](https://pubmed.ncbi.nlm.nih.gov/28319061/)
 14. Tanouchi A, Taniuchi K, Furihata M, Naganuma S, Dabanaka K, Kimura M, Watanabe R, Kohsaki T, Shimizu T, Saito M, Hanazaki K, Saibara T. CCDC88A, a prognostic factor for human pancreatic cancers, promotes the motility and invasiveness of pancreatic cancer cells. *J Exp Clin Cancer Res*. 2016; 35:190.
<https://doi.org/10.1186/s13046-016-0466-0>
PMID:[27919290](https://pubmed.ncbi.nlm.nih.gov/27919290/)
 15. Jiang GY, Zhang XP, Zhang Y, Xu HT, Wang L, Li QC, Wang EH. Coiled-coil domain-containing protein 8 inhibits the invasiveness and migration of non-small cell lung cancer cells. *Hum Pathol*. 2016; 56:64–73.
<https://doi.org/10.1016/j.humpath.2016.06.001>
PMID:[27342910](https://pubmed.ncbi.nlm.nih.gov/27342910/)
 16. Deng JL, Xu YH, Wang G. Identification of potential crucial genes and key pathways in breast cancer using bioinformatic analysis. *Front Genet*. 2019; 10:695.
<https://doi.org/10.3389/fgene.2019.00695>
PMID:[31428132](https://pubmed.ncbi.nlm.nih.gov/31428132/)
 17. Liu YR, Hu Y, Zeng Y, Li ZX, Zhang HB, Deng JL, Wang G. Neurexophilin and PC-esterase domain family member 4 (NXPE4) and prostate androgen-regulated mucin-like protein 1 (PARM1) as prognostic biomarkers for colorectal cancer. *J Cell Biochem*. 2019; 120:18041–52.
<https://doi.org/10.1002/jcb.29107> PMID:[31297877](https://pubmed.ncbi.nlm.nih.gov/31297877/)
 18. Deng JL, Zhang HB, Zeng Y, Xu YH, Huang Y, Wang G. Effects of CORO2A on cell migration and proliferation and its potential regulatory network in breast cancer. *Front Oncol*. 2020; 10:916.
<https://doi.org/10.3389/fonc.2020.00916>
PMID:[32695665](https://pubmed.ncbi.nlm.nih.gov/32695665/)
 19. Geng W, Liang W, Fan Y, Ye Z, Zhang L. Overexpression of CCDC34 in colorectal cancer and its involvement in tumor growth, apoptosis and invasion. *Mol Med Rep*. 2018; 17:465–73.
<https://doi.org/10.3892/mmr.2017.7860>
PMID:[29115580](https://pubmed.ncbi.nlm.nih.gov/29115580/)
 20. Cui L, Liang B, Yang Y, Zhu M, Kwong J, Zheng H, Wang CC. Inhibition of coiled coil domain containing protein 69 enhances platinum-induced apoptosis in ovarian cancer cells. *Oncotarget*. 2017; 8:101634–48.
<https://doi.org/10.18632/oncotarget.21356>
PMID:[29254192](https://pubmed.ncbi.nlm.nih.gov/29254192/)
 21. Ning Y, Wang C, Liu X, Du Y, Liu S, Liu K, Zhou J, Zhou C. CK2-mediated CCDC106 phosphorylation is required for p53 degradation in cancer progression. *J Exp Clin Cancer Res*. 2019; 38:131.
<https://doi.org/10.1186/s13046-019-1137-8>
PMID:[30885251](https://pubmed.ncbi.nlm.nih.gov/30885251/)
 22. Diallo I, Provost P. RNA-sequencing analyses of small bacterial RNAs and their emergence as virulence factors in host-pathogen interactions. *Int J Mol Sci*. 2020; 21:1627.
<https://doi.org/10.3390/ijms21051627>
PMID:[32120885](https://pubmed.ncbi.nlm.nih.gov/32120885/)
 23. Gratton R, Tricarico PM, Agrelli A, Colaço da Silva HV, Coelho Bernardo L, Crovella S, Campos Coelho AV, Rodrigues de Moura R, Cavalcanti Brandão LA. *In vitro* zika virus infection of human neural progenitor cells: meta-analysis of RNA-seq assays. *Microorganisms*. 2020; 8:270.
<https://doi.org/10.3390/microorganisms8020270>
PMID:[32079323](https://pubmed.ncbi.nlm.nih.gov/32079323/)
 24. Bakhoun MF, Esmaeli B. Molecular characteristics of uveal melanoma: insights from the cancer genome atlas (TCGA) project. *Cancers (Basel)*. 2019; 11:1061.
<https://doi.org/10.3390/cancers11081061>
PMID:[31357599](https://pubmed.ncbi.nlm.nih.gov/31357599/)
 25. Wu CC, Ekanem TI, Phan NN, Loan DT, Hou SY, Lee KH,

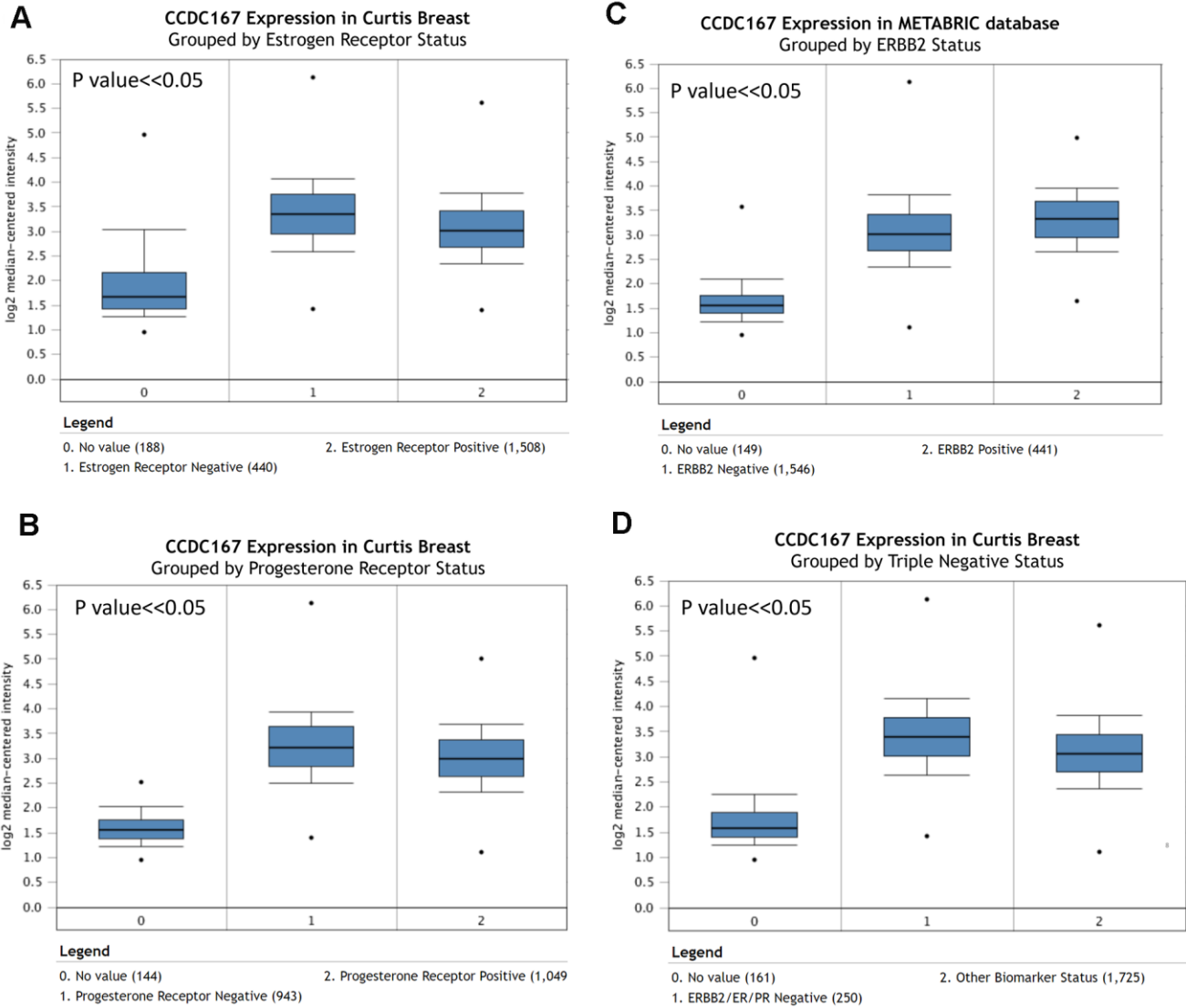
- Wang CY. Gene signatures and prognostic analyses of the Tob/BTG pituitary tumor-transforming gene (PTTG) family in clinical breast cancer patients. *Int J Med Sci.* 2020; 17:3112–24.
<https://doi.org/10.7150/ijms.49652> PMID:33173433
26. Hagerling C, Owyong M, Sitarama V, Wang CY, Lin C, van den Bijgaart RJ, Koopman CD, Brenot A, Nanjaraj A, Wärnberg F, Jirström K, Klein OD, Werb Z, Plaks V. LGR5 in breast cancer and ductal carcinoma in situ: a diagnostic and prognostic biomarker and a therapeutic target. *BMC Cancer.* 2020; 20:542.
<https://doi.org/10.1186/s12885-020-06986-z> PMID:32522170
27. Zeng Y, Wang G, Zhou CF, Zhang HB, Sun H, Zhang W, Zhou HH, Liu R, Zhu YS. LncRNA profile study reveals a three-LncRNA signature associated with the pathological complete response following neoadjuvant chemotherapy in breast cancer. *Front Pharmacol.* 2019; 10:574.
<https://doi.org/10.3389/fphar.2019.00574> PMID:31191314
28. Zhao QQ, Jiang C, Gao Q, Zhang YY, Wang G, Chen XP, Wu SB, Tang J. Gene expression and methylation profiles identified CXCL3 and CXCL8 as key genes for diagnosis and prognosis of colon adenocarcinoma. *J Cell Physiol.* 2020; 235:4902–12.
<https://doi.org/10.1002/jcp.29368> PMID:31709538
29. Hagerling C, Gonzalez H, Salari K, Wang CY, Lin C, Robles I, van Gogh M, Dejmeek A, Jirström K, Werb Z. Immune effector monocyte-neutrophil cooperation induced by the primary tumor prevents metastatic progression of breast cancer. *Proc Natl Acad Sci USA.* 2019; 116:21704–14.
<https://doi.org/10.1073/pnas.1907660116> PMID:31591235
30. Hsu HP, Wang CY, Hsieh PY, Fang JH, Chen YL. Knockdown of serine/threonine-protein kinase 24 promotes tumorigenesis and myeloid-derived suppressor cell expansion in an orthotopic immunocompetent gastric cancer animal model. *J Cancer.* 2020; 11:213–28.
<https://doi.org/10.7150/jca.35821> PMID:31892988
31. Ou KC, Wang CY, Liu KT, Chen YL, Chen YC, Lai MD, Yen MC. Optimization protein productivity of human interleukin-2 through codon usage, gene copy number and intracellular tRNA concentration in CHO cells. *Biochem Biophys Res Commun.* 2014; 454:347–52.
<https://doi.org/10.1016/j.bbrc.2014.10.097> PMID:25451252
32. Liu YL, Chou CK, Kim M, Vasisht R, Kuo YA, Ang P, Liu C, Perillo EP, Chen YA, Blocher K, Horng H, Chen YI, Nguyen DT, et al. Assessing metastatic potential of breast cancer cells based on EGFR dynamics. *Sci Rep.* 2019; 9:3395.
<https://doi.org/10.1038/s41598-018-37625-0> PMID:30833579
33. Lin YY, Wang CY, Phan NN, Chiao CC, Li CY, Sun Z, Hung JH, Chen YL, Yen MC, Weng TY, Hsu HP, Lai MD. PODXL2 maintains cellular stemness and promotes breast cancer development through the Rac1/Akt pathway. *Int J Med Sci.* 2020; 17:1639–51.
<https://doi.org/10.7150/ijms.46125> PMID:32669966
34. Jönsson G, Staaf J, Vallon-Christersson J, Ringnér M, Gruvberger-Saal SK, Saal LH, Holm K, Hegardt C, Arason A, Fagerholm R, Persson C, Grabau D, Johnsson E, et al. The retinoblastoma gene undergoes rearrangements in BRCA1-deficient basal-like breast cancer. *Cancer Res.* 2012; 72:4028–36.
<https://doi.org/10.1158/0008-5472.CAN-12-0097> PMID:22706203
35. Palazon A, Tyrakis PA, Macias D, Veliça P, Rundqvist H, Fitzpatrick S, Vojnovic N, Phan AT, Loman N, Hedenfalk I, Hatschek T, Lövrot J, Foukakis T, et al. An HIF-1 α /VEGF- α axis in cytotoxic T cells regulates tumor progression. *Cancer Cell.* 2017; 32:669–83.e5.
<https://doi.org/10.1016/j.ccell.2017.10.003> PMID:29136509
36. Lundberg A, Lindström LS, Harrell JC, Falato C, Carlson JW, Wright PK, Foukakis T, Perou CM, Czene K, Bergh J, Tobin NP. Gene expression signatures and immunohistochemical subtypes add prognostic value to each other in breast cancer cohorts. *Clin Cancer Res.* 2017; 23:7512–20.
<https://doi.org/10.1158/1078-0432.CCR-17-1535> PMID:28972043
37. Yang Y, Han L, Yuan Y, Li J, Hei N, Liang H. Gene co-expression network analysis reveals common system-level properties of prognostic genes across cancer types. *Nat Commun.* 2014; 5:3231.
<https://doi.org/10.1038/ncomms4231> PMID:24488081
38. Yadav VK, Lee TY, Hsu JB, Huang HD, Yang WV, Chang TH. Computational analysis for identification of the extracellular matrix molecules involved in endometrial cancer progression. *PLoS One.* 2020; 15:e0231594.
<https://doi.org/10.1371/journal.pone.0231594> PMID:32315343
39. van Dam S, Vösa U, van der Graaf A, Franke L, de Magalhães JP. Gene co-expression analysis for functional classification and gene-disease predictions. *Brief Bioinform.* 2018; 19:575–92.
<https://doi.org/10.1093/bib/bbw139> PMID:28077403
40. Wang CY, Chiao CC, Phan NN, Li CY, Sun ZD, Jiang JZ,

- Hung JH, Chen YL, Yen MC, Weng TY, Chen WC, Hsu HP, Lai MD. Gene signatures and potential therapeutic targets of amino acid metabolism in estrogen receptor-positive breast cancer. *Am J Cancer Res.* 2020; 10:95–113. PMID:[32064155](https://pubmed.ncbi.nlm.nih.gov/32064155/)
41. Su YH, Tang WC, Cheng YW, Sia P, Huang CC, Lee YC, Jiang HY, Wu MH, Lai IL, Lee JW, Lee KH. Targeting of multiple oncogenic signaling pathways by Hsp90 inhibitor alone or in combination with berberine for treatment of colorectal cancer. *Biochim Biophys Acta.* 2015; 1853:2261–72. <https://doi.org/10.1016/j.bbamcr.2015.05.012> PMID:[25982393](https://pubmed.ncbi.nlm.nih.gov/25982393/)
 42. Lee KH, Lo HL, Tang WC, Hsiao HH, Yang PM. A gene expression signature-based approach reveals the mechanisms of action of the Chinese herbal medicine berberine. *Sci Rep.* 2014; 4:6394. <https://doi.org/10.1038/srep06394> PMID:[25227736](https://pubmed.ncbi.nlm.nih.gov/25227736/)
 43. Liu TP, Hsieh YY, Chou CJ, Yang PM. Systematic polypharmacology and drug repurposing via an integrated L1000-based connectivity map database mining. *R Soc Open Sci.* 2018; 5:181321. <https://doi.org/10.1098/rsos.181321> PMID:[30564416](https://pubmed.ncbi.nlm.nih.gov/30564416/)
 44. Lv C, Zeng HW, Wang JX, Yuan X, Zhang C, Fang T, Yang PM, Wu T, Zhou YD, Nagle DG, Zhang WD. The antitumor natural product tanshinone IIA inhibits protein kinase C and acts synergistically with 17-AAG. *Cell Death Dis.* 2018; 9:165. <https://doi.org/10.1038/s41419-017-0247-5> PMID:[29416003](https://pubmed.ncbi.nlm.nih.gov/29416003/)
 45. Liu TP, Hong YH, Yang PM. *In silico* and *in vitro* identification of inhibitory activities of sorafenib on histone deacetylases in hepatocellular carcinoma cells. *Oncotarget.* 2017; 8:86168–80. <https://doi.org/10.18632/oncotarget.21030> PMID:[29156785](https://pubmed.ncbi.nlm.nih.gov/29156785/)
 46. Cho CY, Lee KT, Chen WC, Wang CY, Chang YS, Huang HL, Hsu HP, Yen MC, Lai MZ, Lai MD. MST3 promotes proliferation and tumorigenicity through the VAV2/Rac1 signal axis in breast cancer. *Oncotarget.* 2016; 7:14586–604. <https://doi.org/10.18632/oncotarget.7542> PMID:[26910843](https://pubmed.ncbi.nlm.nih.gov/26910843/)
 47. Chen WC, Hsu HP, Li CY, Yang YJ, Hung YH, Cho CY, Wang CY, Weng TY, Lai MD. Cancer stem cell marker CD90 inhibits ovarian cancer formation via $\beta 3$ integrin. *Int J Oncol.* 2016; 49:1881–89. <https://doi.org/10.3892/ijo.2016.3691> PMID:[27633757](https://pubmed.ncbi.nlm.nih.gov/27633757/)
 48. Weng TY, Huang SS, Yen MC, Lin CC, Chen YL, Lin CM, Chen WC, Wang CY, Chang JY, Lai MD. A novel cancer therapeutic using thrombospondin 1 in dendritic cells. *Mol Ther.* 2014; 22:292–302. <https://doi.org/10.1038/mt.2013.236> PMID:[24127010](https://pubmed.ncbi.nlm.nih.gov/24127010/)
 49. Weng TY, Yen MC, Huang CT, Hung JJ, Chen YL, Chen WC, Wang CY, Chang JY, Lai MD. DNA vaccine elicits an efficient antitumor response by targeting the mutant Kras in a transgenic mouse lung cancer model. *Gene Ther.* 2014; 21:888–96. <https://doi.org/10.1038/gt.2014.67> PMID:[25077772](https://pubmed.ncbi.nlm.nih.gov/25077772/)
 50. Weng TY, Wu HF, Li CY, Hung YH, Chang YW, Chen YL, Hsu HP, Chen YH, Wang CY, Chang JY, Lai MD. Homoharringtonine induced immune alteration for an efficient anti-tumor response in mouse models of non-small cell lung adenocarcinoma expressing kras mutation. *Sci Rep.* 2018; 8:8216. <https://doi.org/10.1038/s41598-018-26454-w> PMID:[29844447](https://pubmed.ncbi.nlm.nih.gov/29844447/)
 51. Owyong M, Chou J, van den Bijgaart RJ, Kong N, Efe G, Maynard C, Talmi-Frank D, Solomonov I, Koopman C, Hadler-Olsen E, Headley M, Lin C, Wang CY, et al. MMP9 modulates the metastatic cascade and immune landscape for breast cancer anti-metastatic therapy. *Life Sci Alliance.* 2019; 2:e201800226. <https://doi.org/10.26508/lsa.201800226> PMID:[31727800](https://pubmed.ncbi.nlm.nih.gov/31727800/)
 52. Rhodes DR, Yu J, Shanker K, Deshpande N, Varambally R, Ghosh D, Barrette T, Pandey A, Chinnaiyan AM. ONCOMINE: a cancer microarray database and integrated data-mining platform. *Neoplasia.* 2004; 6:1–6. [https://doi.org/10.1016/s1476-5586\(04\)80047-2](https://doi.org/10.1016/s1476-5586(04)80047-2) PMID:[15068665](https://pubmed.ncbi.nlm.nih.gov/15068665/)
 53. Wang CY, Li CY, Hsu HP, Cho CY, Yen MC, Weng TY, Chen WC, Hung YH, Lee KT, Hung JH, Chen YL, Lai MD. PSMB5 plays a dual role in cancer development and immunosuppression. *Am J Cancer Res.* 2017; 7:2103–20. PMID:[29218236](https://pubmed.ncbi.nlm.nih.gov/29218236/)
 54. Wang CY, Chang YC, Kuo YL, Lee KT, Chen PS, Cheung CH, Chang CP, Phan NN, Shen MR, Hsu HP. Mutation of the PTCH1 gene predicts recurrence of breast cancer. *Sci Rep.* 2019; 9:16359. <https://doi.org/10.1038/s41598-019-52617-4> PMID:[31704974](https://pubmed.ncbi.nlm.nih.gov/31704974/)
 55. Cheng LC, Chao YJ, Overman MJ, Wang C, Phan NN, Chen YL, Wang TW, Hsu HP, Shan YS, Lai MD. Increased expression of secreted frizzled related protein 1 (SFRP1) predicts ampullary adenocarcinoma recurrence. *Sci Rep.* 2020; 10:13255. <https://doi.org/10.1038/s41598-020-69899-8> PMID:[32764696](https://pubmed.ncbi.nlm.nih.gov/32764696/)

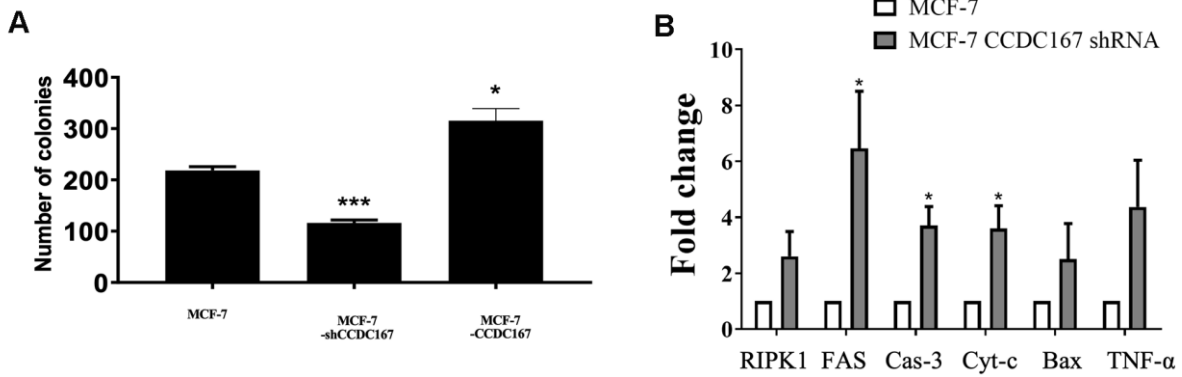
56. Cheng LC, Chao YJ, Wang CY, Phan NN, Chen YL, Wang TW, Hsu HP, Lin YJ, Shan YS, Lai MD. Cancer-derived transforming growth factor- β modulates tumor-associated macrophages in ampullary cancer. *Onco Targets Ther.* 2020; 13:7503–16.
<https://doi.org/10.2147/OTT.S246714>
PMID:[32821120](https://pubmed.ncbi.nlm.nih.gov/32821120/)
57. Cooke DL, McCoy DB, Halbach VV, Hetts SW, Amans MR, Dowd CF, Higashida RT, Lawson D, Nelson J, Wang CY, Kim H, Werb Z, McCulloch C, et al. Endovascular biopsy: *in vivo* cerebral aneurysm endothelial cell sampling and gene expression analysis. *Transl Stroke Res.* 2018; 9:20–33.
<https://doi.org/10.1007/s12975-017-0560-4>
PMID:[28900857](https://pubmed.ncbi.nlm.nih.gov/28900857/)
58. Gao GF, Parker JS, Reynolds SM, Silva TC, Wang LB, Zhou W, Akbani R, Bailey M, Balu S, Berman BP, Brooks D, Chen H, Cherniack AD, et al. Before and After: Comparison of Legacy and Harmonized TCGA Genomic Data Commons' Data. *Cell Syst.* 2019; 9:24–34.e10.
<https://doi.org/10.1016/j.cels.2019.06.006>
PMID:[31344359](https://pubmed.ncbi.nlm.nih.gov/31344359/)
59. Tang Z, Kang B, Li C, Chen T, Zhang Z. GEPIA2: an enhanced web server for large-scale expression profiling and interactive analysis. *Nucleic Acids Res.* 2019; 47:W556–60.
<https://doi.org/10.1093/nar/gkz430> PMID:[31114875](https://pubmed.ncbi.nlm.nih.gov/31114875/)
60. Cancer Genome Atlas Network. Comprehensive molecular portraits of human breast tumours. *Nature.* 2012; 490:61–70.
<https://doi.org/10.1038/nature11412>
PMID:[23000897](https://pubmed.ncbi.nlm.nih.gov/23000897/)
61. Curtis C, Shah SP, Chin SF, Turashvili G, Rueda OM, Dunning MJ, Speed D, Lynch AG, Samarajiwa S, Yuan Y, Gräf S, Ha G, Haffari G, et al, and METABRIC Group. The genomic and transcriptomic architecture of 2,000 breast tumours reveals novel subgroups. *Nature.* 2012; 486:346–52.
<https://doi.org/10.1038/nature10983>
PMID:[22522925](https://pubmed.ncbi.nlm.nih.gov/22522925/)
62. Cerami E, Gao J, Dogrusoz U, Gross BE, Sumer SO, Aksoy BA, Jacobsen A, Byrne CJ, Heuer ML, Larsson E, Antipin Y, Reva B, Goldberg AP, et al. The cBio cancer genomics portal: an open platform for exploring multidimensional cancer genomics data. *Cancer Discov.* 2012; 2:401–04.
<https://doi.org/10.1158/2159-8290.CD-12-0095>
PMID:[22588877](https://pubmed.ncbi.nlm.nih.gov/22588877/)
63. Liu HL, Yeh IJ, Phan NN, Wu YH, Yen MC, Hung JH, Chiao CC, Chen CF, Sun Z, Jiang JZ, Hsu HP, Wang CY, Lai MD. Gene signatures of SARS-CoV/SARS-CoV-2-infected ferret lungs in short- and long-term models. *Infect Genet Evol.* 2020; 85:104438.
<https://doi.org/10.1016/j.meegid.2020.104438>
PMID:[32615317](https://pubmed.ncbi.nlm.nih.gov/32615317/)
64. Sun Z, Wang CY, Lawson DA, Kwek S, Velozo HG, Owyong M, Lai MD, Fong L, Wilson M, Su H, Werb Z, Cooke DL. Single-cell RNA sequencing reveals gene expression signatures of breast cancer-associated endothelial cells. *Oncotarget.* 2017; 9:10945–61.
<https://doi.org/10.18632/oncotarget.23760>
PMID:[29541388](https://pubmed.ncbi.nlm.nih.gov/29541388/)
65. Phan NN, Wang CY, Lin YC. The novel regulations of MEF2A, CAMKK2, CALM3, and TNNI3 in ventricular hypertrophy induced by arsenic exposure in rats. *Toxicology.* 2014; 324:123–35.
<https://doi.org/10.1016/j.tox.2014.07.010>
PMID:[25089838](https://pubmed.ncbi.nlm.nih.gov/25089838/)
66. Thuy TD, Phan NN, Wang CY, Yu HG, Wang SY, Huang PL, Do YY, Lin YC. Novel therapeutic effects of sesamin on diabetes-induced cardiac dysfunction. *Mol Med Rep.* 2017; 15:2949–56.
<https://doi.org/10.3892/mmr.2017.6420>
PMID:[28358428](https://pubmed.ncbi.nlm.nih.gov/28358428/)
67. Kassambara A, Kassambara MA. (2020). Package 'ggpubr'.
68. Györfy B, Lanczky A, Eklund AC, Denkert C, Budczies J, Li Q, Szallasi Z. An online survival analysis tool to rapidly assess the effect of 22,277 genes on breast cancer prognosis using microarray data of 1,809 patients. *Breast Cancer Res Treat.* 2010; 123:725–31.
<https://doi.org/10.1007/s10549-009-0674-9>
PMID:[20020197](https://pubmed.ncbi.nlm.nih.gov/20020197/)

SUPPLEMENTARY MATERIALS

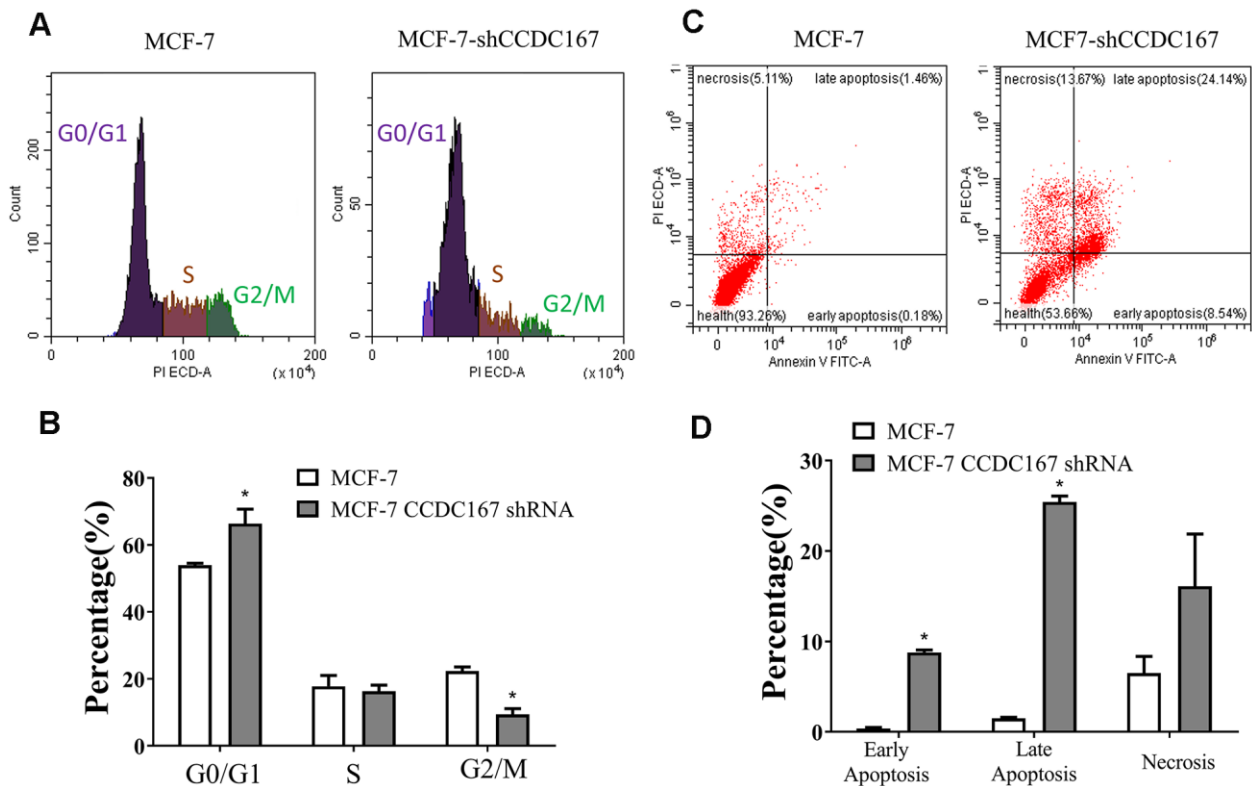
Supplementary Figures



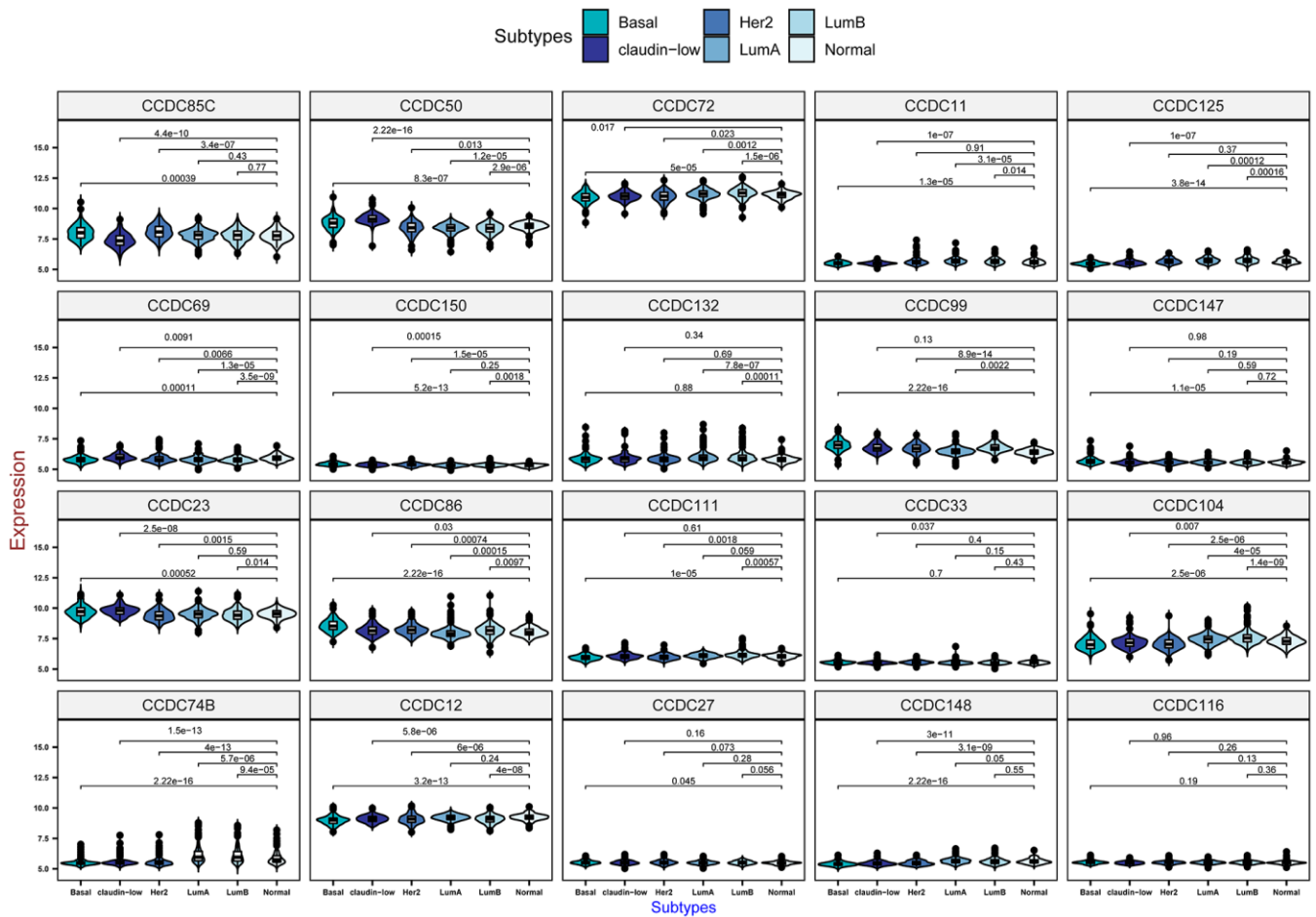
Supplementary Figure 1. Coiled-coil domain-containing protein 167 (CCDC167) expression in the METABRIC database (A) CCDC167 expression in estrogen receptor-positive (ER⁺) breast cancer patients, (B) CCDC167 expression in progesterone receptor-positive (PR⁺) breast cancer patients, (C) CCDC167 expression in ERBB2⁺ (human epidermal growth factor receptor (HER)-2-enriched) breast cancer patients, and (D) CCDC167 expression in triple-negative breast cancer (TNBC) patients.



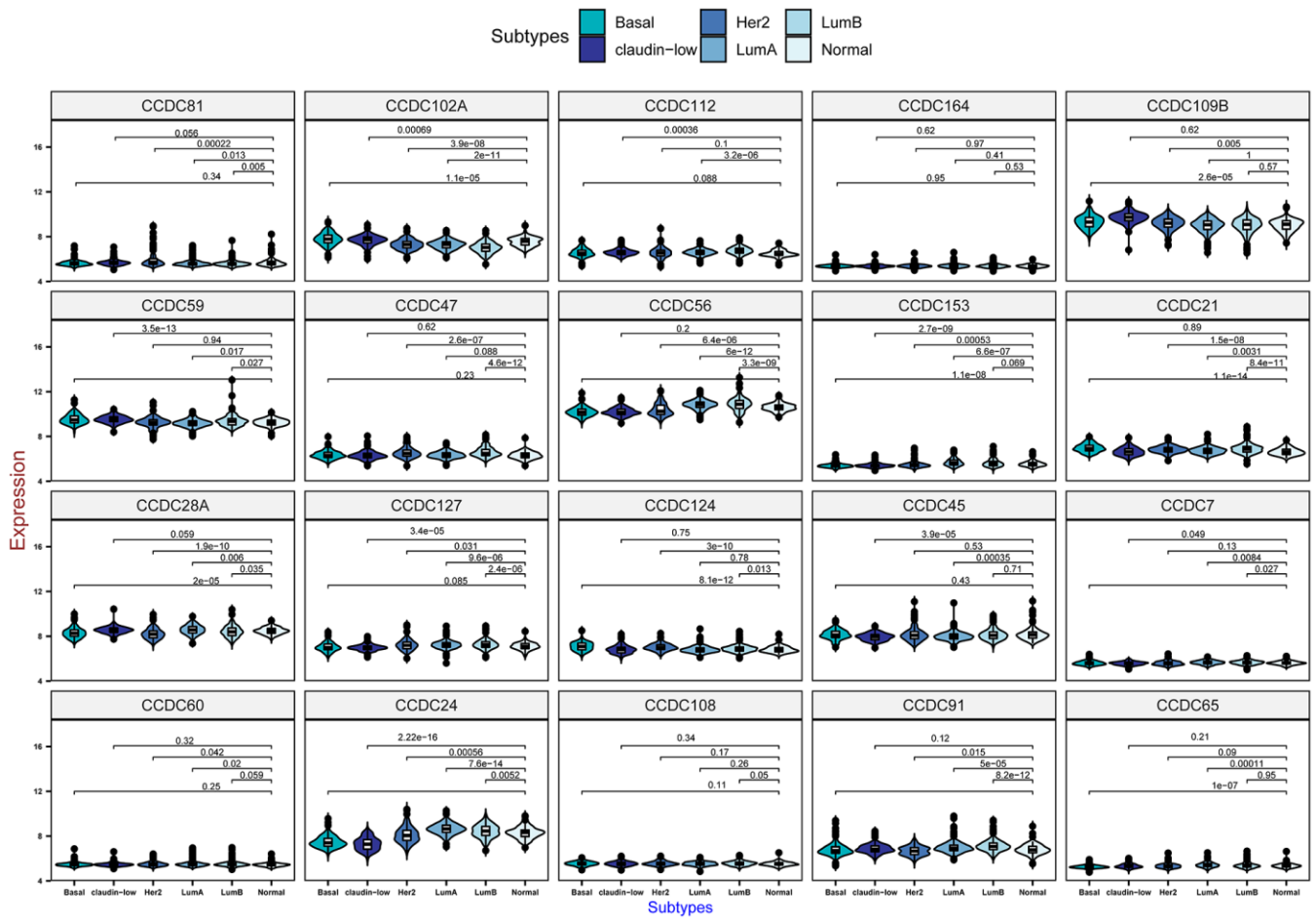
Supplementary Figure 2. Knockdown of coiled-coil domain-containing protein 167 (CCDC167) attenuates cellular growth by regulating cell cycle-related genes (A) Proliferation rates of the MCF-7 control cell line and shCCDC167-knockdown and CCDC167-overexpressing cells were determined by a colony-formation assay. (B) Knockdown of CCDC167 in MCF-7 cells increased apoptosis and necrosis-related gene expressions according to a qPCR.



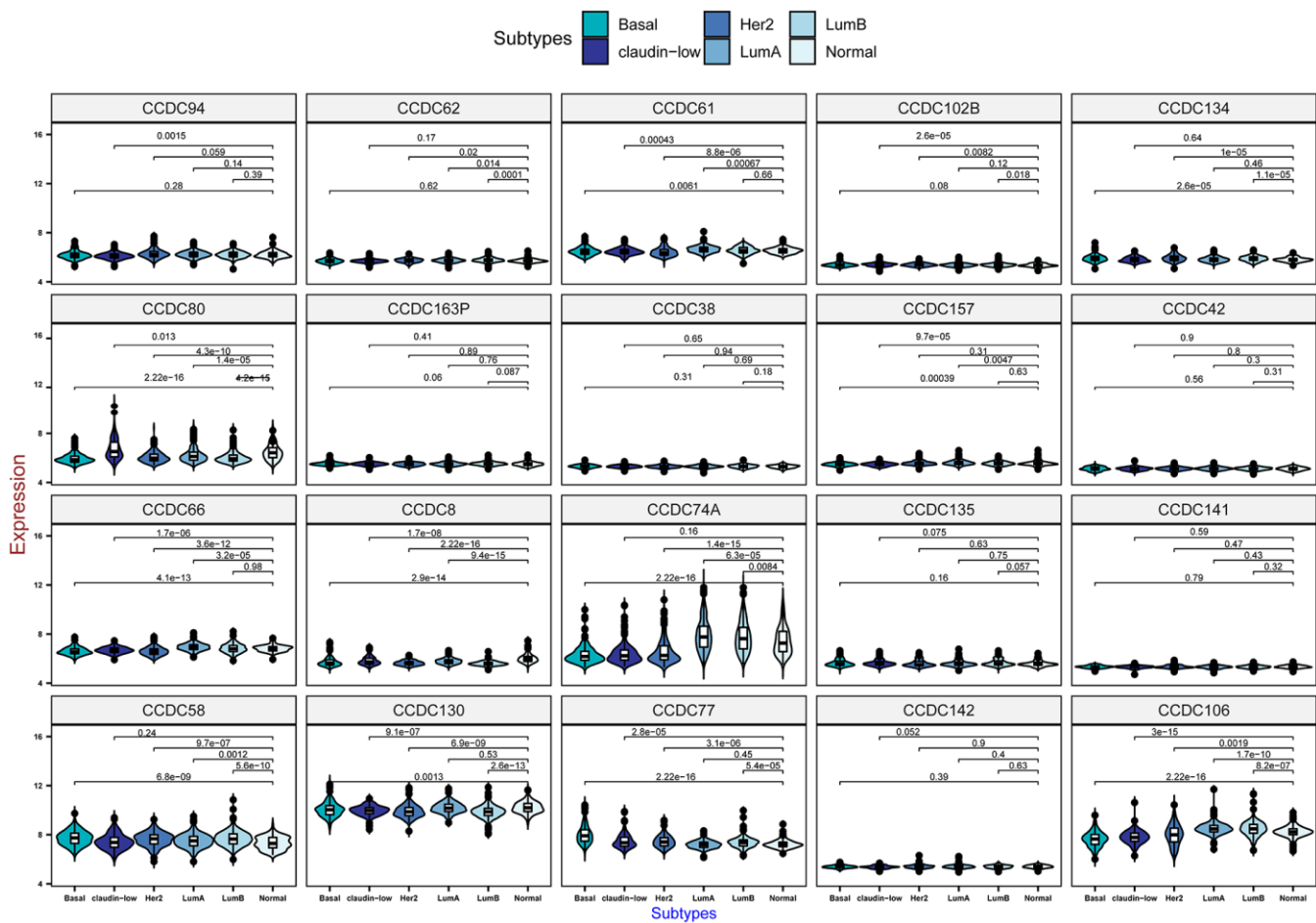
Supplementary Figure 3. Flow cytometric analysis of the cell cycle distribution and apoptosis. (A) The increment in the proportion of cells arrested in the G₀/G₁ phase after knockdown of coiled-coil domain-containing protein 167 (CCDC167) in MCF7 cells. (B) Statistical data of the cell cycle distribution from flow cytometry. (C) Knockdown of CCDC167 initiated early and late apoptotic states and necrotic states compared to the control group. (D) Statistical data of the apoptosis status from flow cytometry.



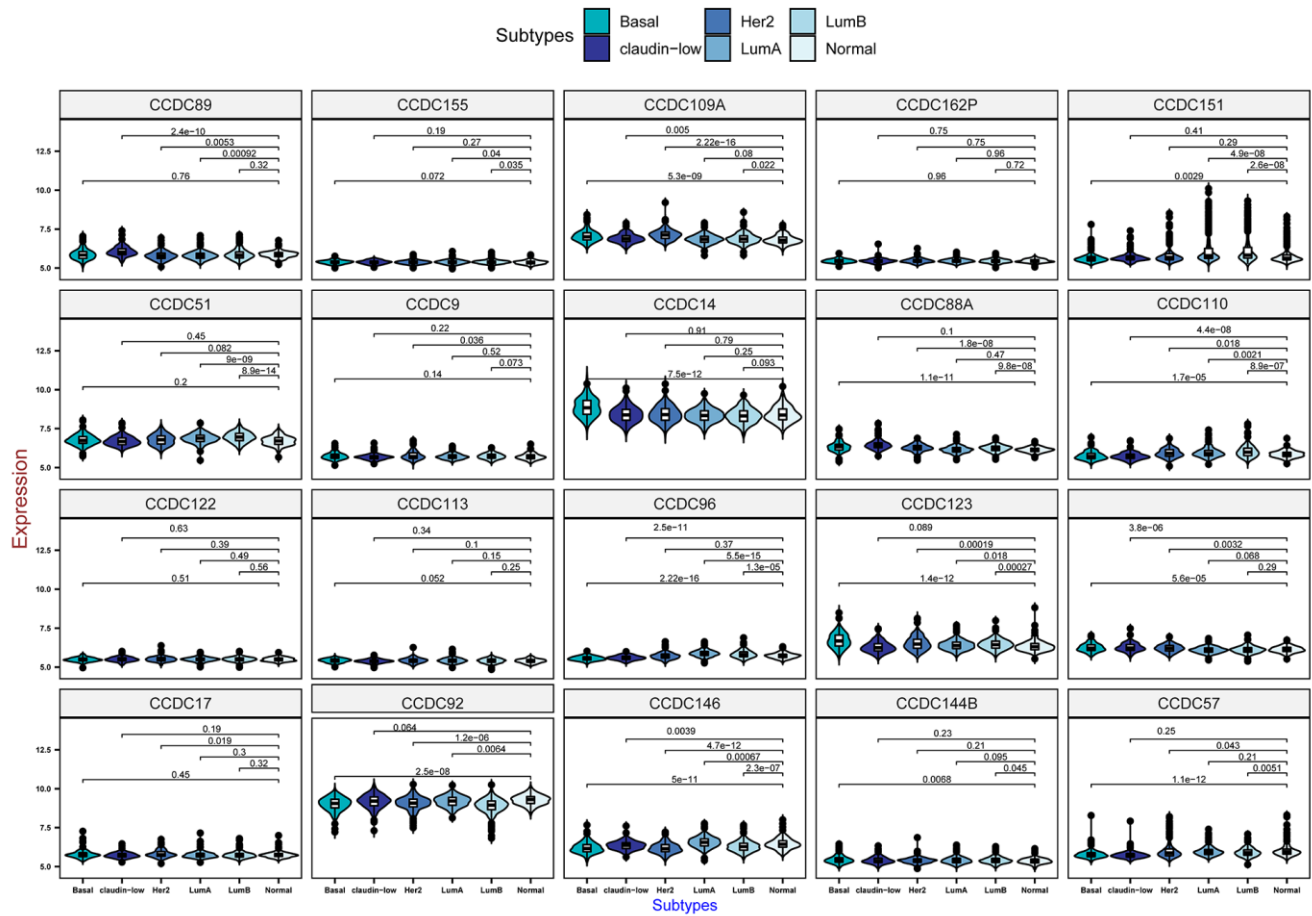
Supplementary Figure 4. Coiled-coil domain-containing protein (CCDC) family gene expressions in the METABRIC database. Comparison of members of the CCDC family in different subtypes of breast cancer (part-1).



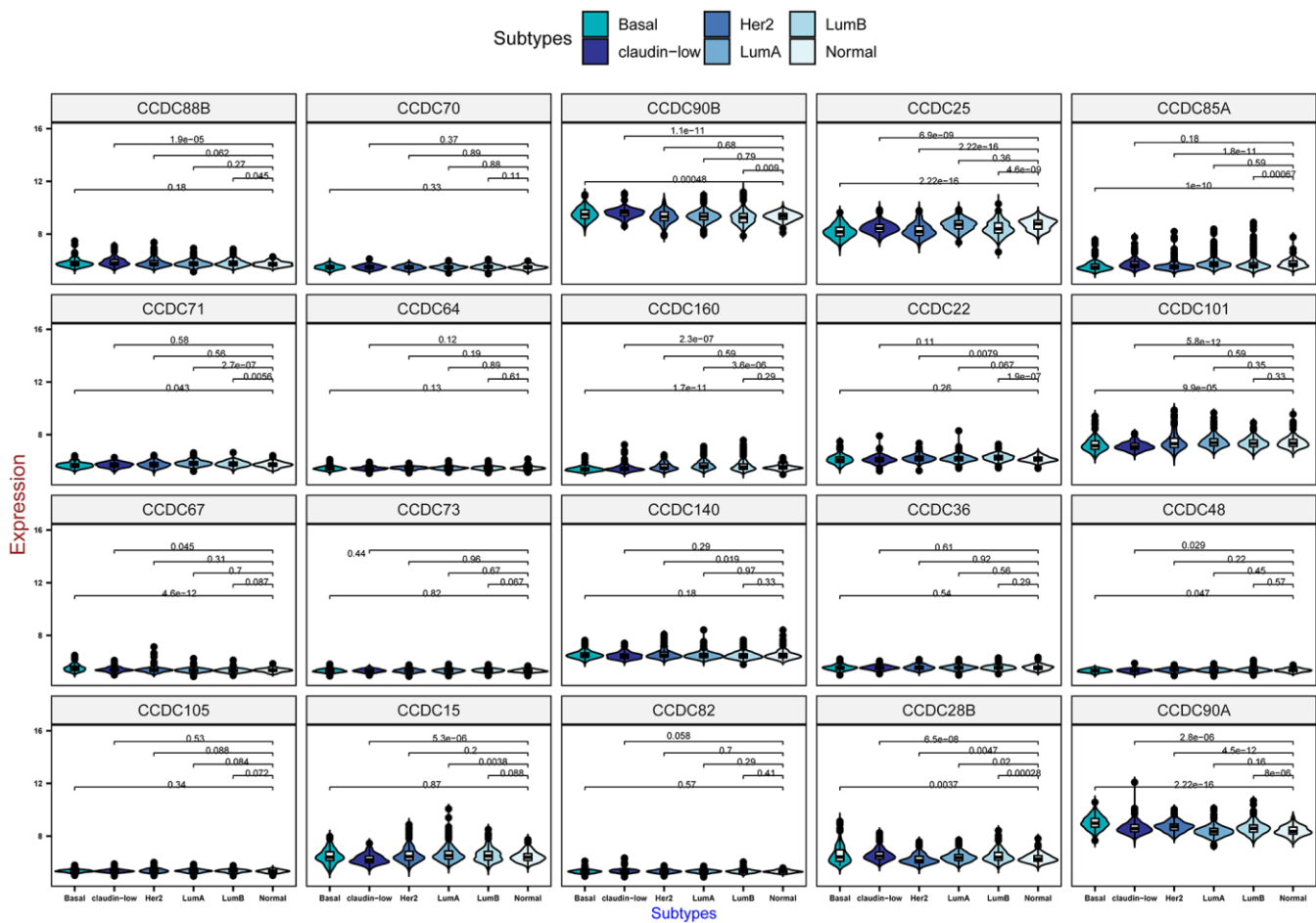
Supplementary Figure 5. The CCDC family gene expression in METABRIC database. Comparison of members of CCDC family in different subtypes of breast cancer (part-2).



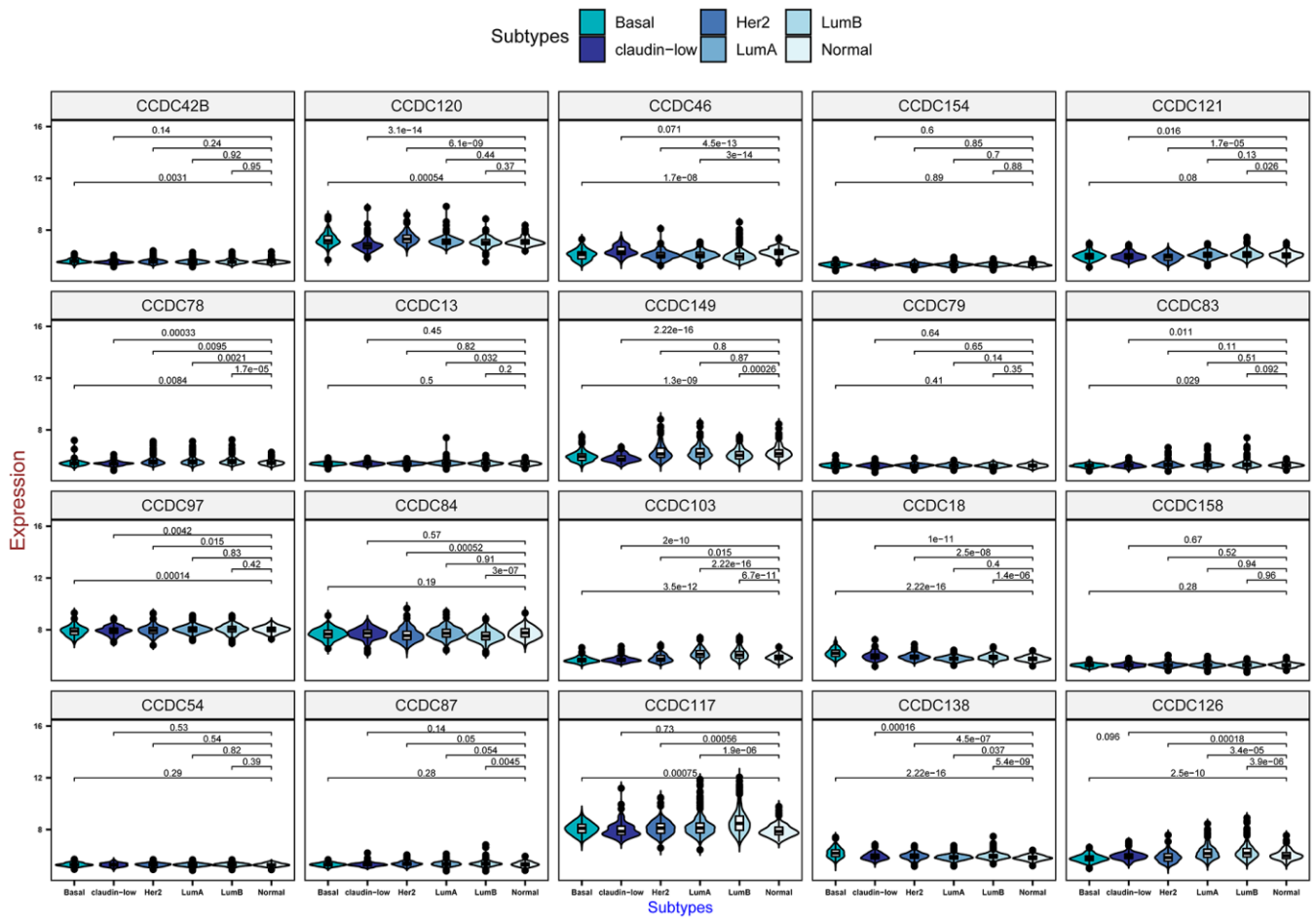
Supplementary Figure 6. The CCDC family gene expression in METABRIC database. Comparison of members of CCDC family in different subtypes of breast cancer (part-3).



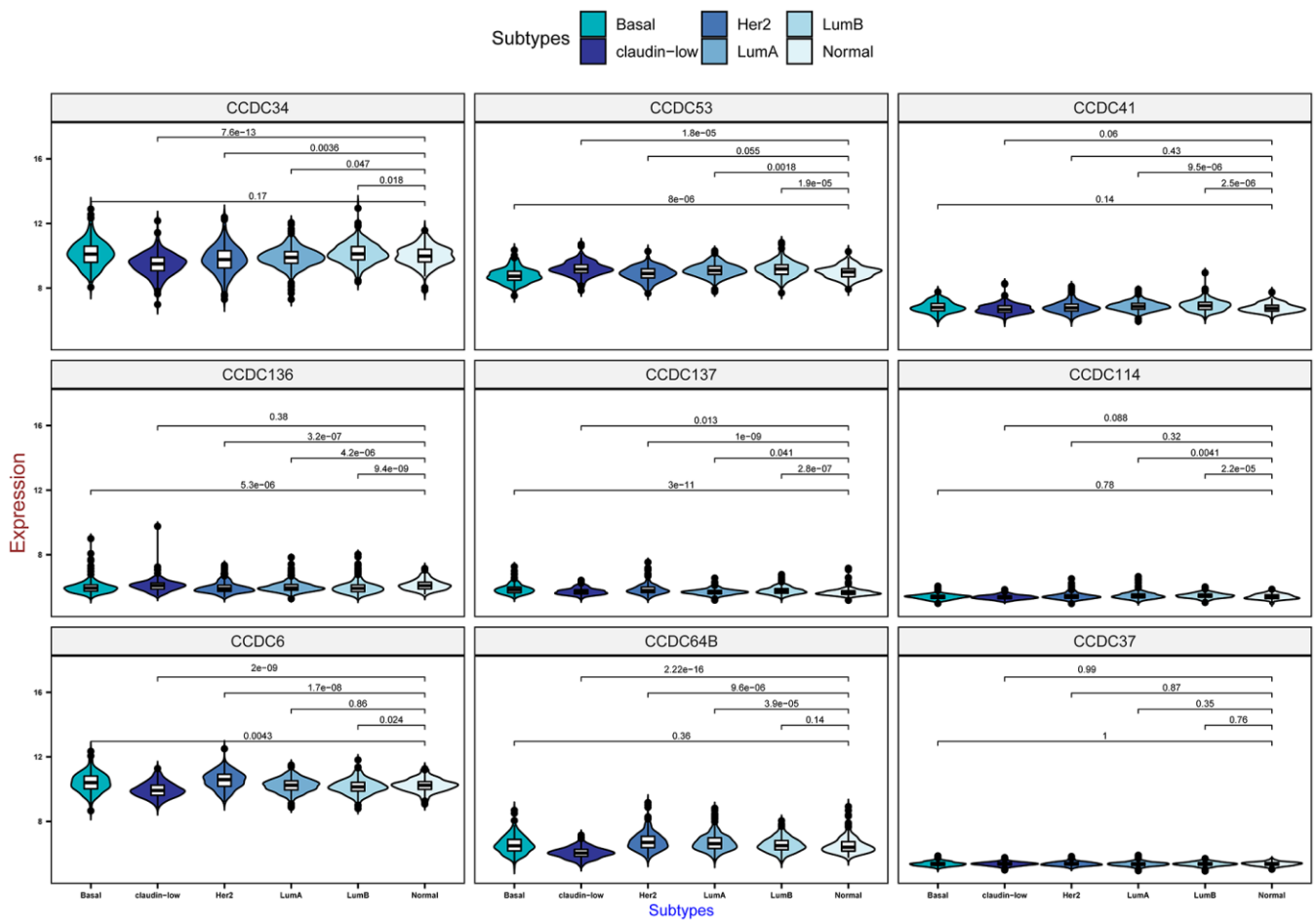
Supplementary Figure 7. The CCDC family gene expression in METABRIC database. Comparison of members of CCDC family in different subtypes of breast cancer (part-4).



Supplementary Figure 8. The CCDC family gene expression in METABRIC database. Comparison of members of CCDC family in different subtypes of breast cancer (part-5).



Supplementary Figure 9. The CCDC family gene expression in METABRIC database. Comparison of members of CCDC family in different subtypes of breast cancer (part-6).



Supplementary Figure 10. The CCDC family gene expression in METABRIC database. Comparison of members of CCDC family in different subtypes of breast cancer (part-7).

Supplementary Table

Please browse Full Text version to see the data of Supplementary Table 1.

Supplementary Table 1. Pathway analysis of 945 common coiled-coil domain-containing protein 167 (CCDC167)-co-expressed genes from TCGA and METABRIC databases using the MetaCore database (with $p < 0.01$ set as the cutoff value).